NTNU

Norwegian University of
Science and Technology

Electrodeposition of Metal Oxides for Solar Cell Applications

Anna Maren Andersen Fyhn

Master of Science in Physics and Mathematics
Submission date: Januar 2012
Supervisor: Ursula Gibson, IFY

Norwegian University of Science and Technology
Department of Physics

Abstract

This thesis investigates the electrodeposition process of zinc-, copper-, silver-, and silver copper oxides at cathodic and anodic voltages. Silver copper oxide has been successfully electrodeposited on a substrate of PtSi from a pH 12 dilute solution of copper nitrate, silver nitrate and sodium hydroxide at 0.9V vs a silver metal cathode. This film was confirmed to be polycrystalline $AgCuO_2$ by EDS and XRD studies. Zinc oxide and copper oxide were deposited on gold substrates from their respective nitrates. The zinc oxide deposition was confirmed polycrystalline in XRD and had a band gap between 3.2eV and 3.5eV measured by optical reflectance. The copper oxide appeared polycrystalline in SEM but only amorphous signal was achieved in XRD, the material had a band gap of around 2eV. Despite many attempts, clean silver oxide was not successfully deposited. These materials may all be suitable for solar cells applications.

Samandrag

Denne oppgåva undersøkjer elektrodeponeringsprosessen for sink-, kopar-, sølv- og sølv-koparoksid under katodiske og anodiske spenningar. Sølv-koparoksid vart vellykka elektrodeponert på eit substrat av PtSi frå ei uttynna løysing av koparnitrat, sølvnitrat og natriumhydroksid ved pH 12 under 0.9V mot ein katode av metallisk sølv. Denne filmen vart stadfesta å vere $AgCuO_2$ av undersøkjingar gjort ved EDS og XRD. Sinkoksid og koparoksid vart deponerte på gullsubstrat frå løysingar av høvesvis sink- og koparnitrat. Sinkoksidfilmen vart stadfesta å vere polykrystallinsk sinkoksid ved XRD og hadde bandgap på mellom 3.2eV og 3.5eV målt ved refleksjon. Koparoksidet var ei blanding mellom Cu_2O og CuO. På trass av mange forsøk vart det ingen deponeringar av reint sølvoksid. Desse materiala kan ha bruksområde i solceller.

Preface

This thesis is written as the final part of my masters degree in Applied Physics and Mathematics at the Norwegian University of Science and Technology (NTNU). Much of the work in this thesis is in electrochemistry, a field in which I have not worked much before. This led to many interesting challenges, like learning to use a potentiostat and finding an appropriate reference electrode. The characterization of the films taught me to interpret results from SEM, EDS, XRD and optical reflectance.

I would like to thank my supervisor professor Ursula Gibson for her patience, enthusiasm and great advice, both in the lab and during the writing of the thesis. Also thanks to phd student Fredrik Martinsen and postdoc Xiaodong Yang for help with EDS and XRD measurements, respectively. Further thanks go to my family for their encouragement, and to Karin for the coffee breaks. Finally thanks to John, without whom I had never gotten this far.

1. Introduction

Solar cells are considered a promising option in today's search for suitable replacements for fossil fuels to counter global warming. Modern day solar cells are for the most part silicon based first generation solar cells. These cells work reasonably well and the technology is well known, but there are a number of drawbacks to current silicon-based solar cells. For one they are single band gap cells. This means that light with less energy than the band-gap will pass right through. For light with higher energy, the extra energy will not be exploited, but rather become heat. The heat in turn reduces the efficiency of the solar cell. Heat is also a problem in Si cells because Si is an indirect band gap semiconductor, so that in order for an electron to be excited into the conduction band heat has to be released. There is also a problem with the production process being environmentally harmful [1].

There are many approaches to finding new photovoltaic cells, the ideal cell being both inexpensive, easy, and environmentally safe to produce with high efficiency and long lifetime. The highest efficiencies measured are around 25% for crystalline Si and GaAs cells. Thin film chalcogenide cells reach 16-19% efficiency, while dye-sensitized solar cells only reach about 10% efficiency. Multijunction- and tandem cells have reached efficiencies higher than 30%, while concentrator cells are the most efficient at 40% [2].

A thin film heterojunction solar cell consists of a large band gap window material in a p-n junction with a small band gap absorption layer. These two materials should ideally have matching lattices, be environmentally friendly and cheap to produce. Zinc oxide is an environmentally friendly, low cost, large band gap material that can easily be produced by electrodeposition [3, 4, 5, 6]. It has been used in heterojunction formation with Cu_2O as the absorption layer [7, 8, 9, 10], but with disappointing results. Another promising material for absorption layer is the newly discovered $AgCuO_2$, or $Ag_2Cu_2O_4$. $AgCuO_2$ has a very low direct band gap, estimated to 0.2eV-0.7eV [32], and consists of materials that are relatively abundant.

For this material to be applied in thin film solar cells, it has to be deposited as a homogeneous thin film in an easy fashion, for example by electrodeposition. This method is both simple and scalable for industrial uses, as it does not require either vacuum or even large voltages. This thesis presents the first electrodeposition of $Ag_2Cu_2O_4$ as a smooth polycrystalline film.

Contents

2. Background

2.1 Semiconductors

Every atom has different discrete energy states, and from the pauli exclusion principle two electrons cannot be in the same state at the same time. When many atoms are brought together in a solid, continuous bands are formed by the adjusted energy levels with a forbidden band between them. At 0K an insulator or semiconductor has a band structure where a completely empty conduction band is separated from a filled valence band by the forbidden gap, see Fig. 2.1 [11]. When the allowed

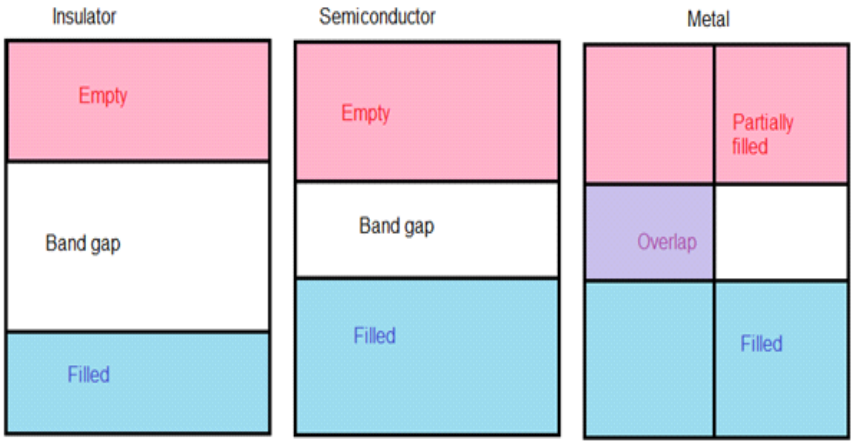

Figure 2.1: Band structure at 0K of insulator, semiconductor and metal. A metal can have either overlapping bands or partially filled conduction band [11].

energy states are plotted against the wave vector ($\vec{k}$)-space the lowest excitation energy is between the lowest point in the conduction band and the highest point in the valence band. When these points are located at the same place along the $\vec{k}$-axis, it is called a direct band gap, while when they are not, it is called an indirect band gap. Direct band gaps are associated with optical transistions,

because photon momentum is very small. In an indirect band gap material, a phonon (carrying momentum) is required for transition between the bands, as shown in Fig. 2.2. A phonon also carries energy. The electron may go via a defect state within the band gap to get to the appropriate $\vec{k}$-position for direct excitation/recombination; this state is called a virtual state, and the electron waits in this state for a phonon of the right energy. The two-step excitation process decreases the transition probability compared to a direct band gap one-step transition [12], thus decreasing the optical response of the material.
A semiconductor is like an insulator, but with a smaller band gap, typically less than 3eV. An undoped semiconductor is called intrinsic. By insertion of impurities, a semiconductor can be doped, creating an extrinsic semiconductor [13]. The Fermi level is the potential energy level where a (hypothetical) electron state would have a 50% probability of being occupied at thermal equilibrium. For an intrinsic semiconductor the Fermi level is in the middle of the band gap, as the number of occupied states in the conduction band equals the number of unoccupied states in the valence band. If the semiconductor is doped, the concentration of holes in the valence band or of electrons in the conduction band can be made higher. The two types of doping are called p- and n-doping, respectively. The p-side is a semiconductor doped with a material with fewer occupied electron states than the original material (e.g. B in Si), which gives rise to free electron states called "holes". A hole moves by being occupied by a neighboring electron, leaving an empty state behind in the electron's previous location (now a hole). N-type material is created by doping the semiconductor

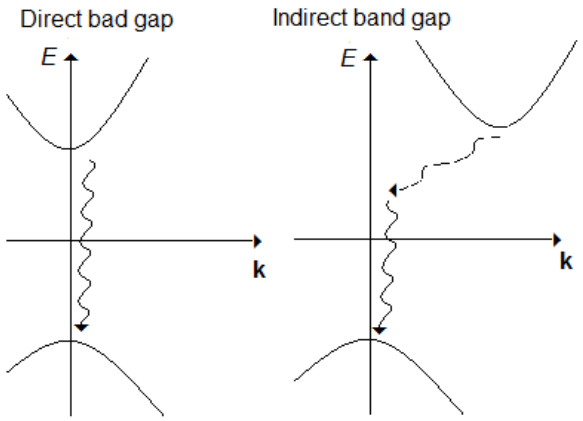

Figure 2.2: direct and indirect band gaps [13].

with a material with one more occupied electron state (e.g. P in Si). Electrons move by occupying neighboring unoccupied states. This means that a p-type material has high a concentration of mobile holes in the valence band and a low electron concentration in the conduction band while the opposite is true for an n-type material. The p- and n- type materials are however not electrically charged [11]. Some materials are spontaneously n- or p-type due to structural defects acting as dopants, for example is ZnO n-type because of Zn interstitials and O vacancies [14].

The Fermi level moves closer to the valence band when the material is p-doped, and closer to the conduction band for a n-doped material (see Fig. 2.3) to compensate for the doping-induced changes in concentration of occupied states [11].

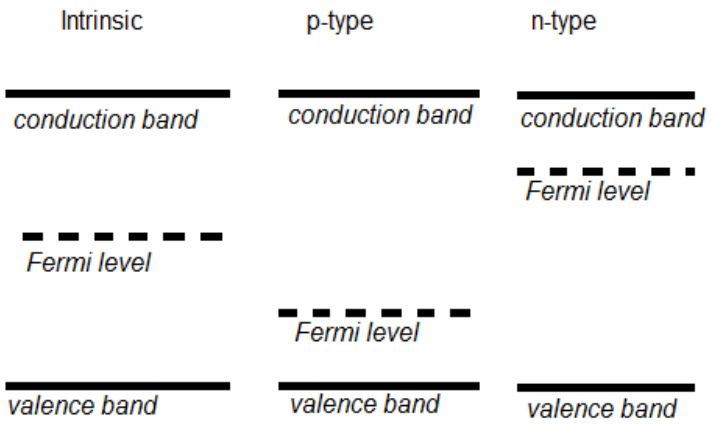

Figure 2.3: Fermi levels for intrinsic, p- doped and n-doped semiconductors [11].

2.1.1 p-n junctions

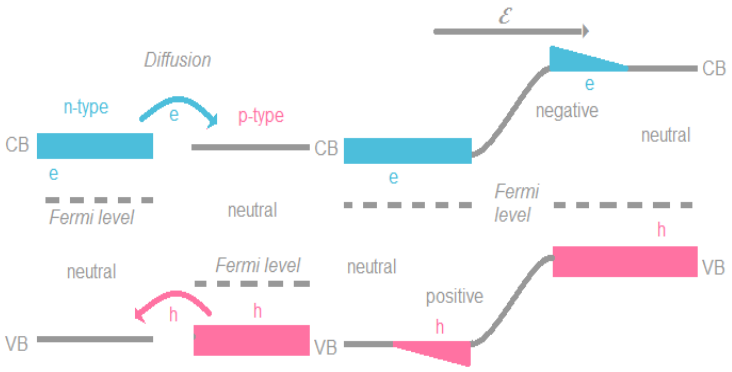

Figure 2.4: The p-type material has a higher concentration of holes, and the n-type material has a higher concentration of electrons. When the two are brought into contact this gives rise to diffusion of carriers, which in turn gives rise to a potential difference across the junction [11].

When a p- and an n-type material are brought into contact, differences in concentrations of holes

and electrons between the materials will lead to diffusion across the junction. Holes diffuse from the p-type material into the n-type material and electrons from the n-type into the p-type material. The diffusion causes the regions closest to the junction on both sides to be electrically charged. This difference in charge in turn gives rise to an electric field across the junction. The electric field then counters the diffusion caused by difference in hole and electron concentration, and equilibrium is obtained. The Fermi levels align, because when there is thermal equilibrium there can only be one Fermi level. Thus a junction is formed. A homojunction is a junction where the p- and n- sides are the same material, and a heterojunction is a junction where they are of different materials. An illustration of this process is shown in Fig. 2.4.

2.2 Solar cells

A solar cell absorbs light and transforms it into electrical power. Semiconductor solar cells are p-n junctions where the light is absorbed in the junction. The solar energy distribution peaks around 500nm wavelength, as the spectrum follows the black body radiation from a 6000K source like the sun see Fig. 2.5 a) [15]. The energy of a photon depends on the wavelength according to Equation 2.1.

$$E_{photon} = h\nu = \frac{hc}{\lambda} \tag{2.1}$$

This means that for light of 500nm, the photon energy is 2.5eV. Most of the photons come at 1eV [13]. They have less energy per photon, therefore the difference in peak location from the energy distribution. If the photon energy is higher than the band gap of a semiconductor, it is absorbed by exciting an electron. For low band gap semiconductors more photons will be absorbed, but the excess energy will not be exploited. For higher band gap semiconductors there will be less excess energy, but fewer photons will be absorbed. Good band gaps for solar absorption are therefore around 1eV, as these wavelengths absorb most of the photons without to much excess energy.

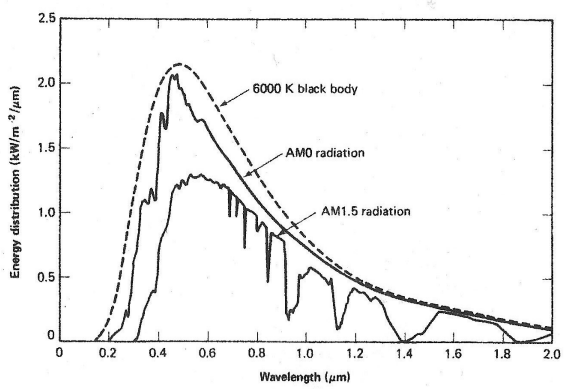

Figure 2.5: The solar radiance spectrum. The figure is from [15].

2.2.1 p-n homojunction solar cells

When light shines onto a semiconductor it can be either reflected, transmitted or absorbed. If it is not reflected from the surface, it will enter the semiconductor. There, in general, photons with energy

higher than the semiconductor band gap will be absorbed, whereas the rest will be transmitted. When a photon with sufficiently high energy enters a semiconductor it will be absorbed by exciting an electron from the valence band to the conduction band, thus creating an electron-hole pair. When the electron-hole pair is created it must not be allowed to recombine directly, as this would only create another photon and possibly heat, instead of electrical energy. The built-in electric field of the p-n junction can separate them spatially. A current is created if the separated charge carriers diffuse towards the contacts. When the device is illuminated, the light-generated current causes the $I - V$ curve to be displaced downward (more negative current). The dark characteristics of a p-n

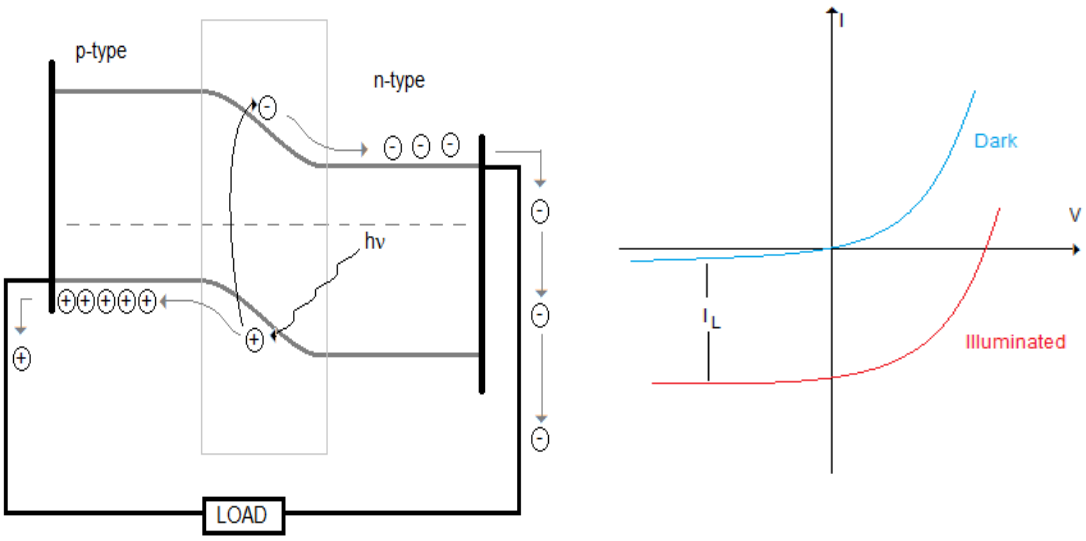

Figure 2.6: Band diagram and dark and illuminated $I - V$ characteristics of a p-n homojunction solar cell [15].

junction solar cell are those of a p-n junction diode. The light generated current is collected within a minority carrier diffusion length of the p-n junction depletion region [15], see Fig. 2.6.

2.2.2 Homojunctions and heterojunctions

Homojunctions typically need a shallow junction in order to achieve short wavelength response. To reduce the series resistance in the top layer it needs to be heavily doped, as doping increases the number of charge carriers. This in turn will reduce the minority carrier diffusion length by increasing the recombination in this layer. Recombination at the surface occurs due to surface states [12]. The

most common commercial solar cells are made of silicon, which is an indirect band gap semiconductor [11]. In order to develop a non-toxic, effective type of p-n solar cells, new materials are being explored. Not all these materials can conveniently be doped both p- and n-type, and in order to make a p-n junction with the desired compounds it is sometimes necessary to create a heterojunction. A

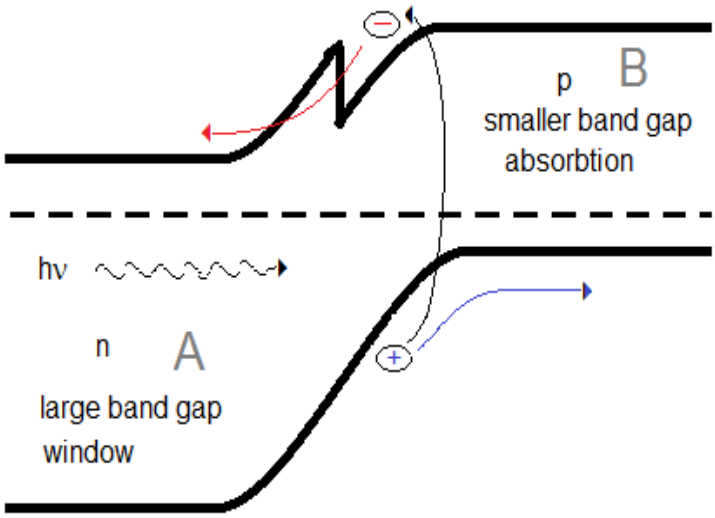

Figure 2.7: A heterojunction between a wide band gap n-type window layer and a narrow band gap p-type absorber with a discontinuity spike in the conduction band [16].

heterojunction cell consists of two different semiconductors with different band gaps, here generalized as material A and material B. Material A has the wider band gap and acts as a window layer where all photons with energy below the material A band gap are passed through. These photons are in turn absorbed in the depletion region or close to it in material B, the absorption layer [12]. The window layer does not absorb any photons itself. The primary function of this layer is to allow as much light as possible to pass through to the junction and material B [16]. The junction and the absorption layer perform the absorption. A good absorption material should have a high absorption coefficient, because only the excitons created in or near the junction can be harvested. The band gap should be small and direct, and the two materials should have a minimum of interface defects [16]. Because material A and B are different there is a difference in structure, lattice spacing and band gaps. The difference in band gaps creates discontinuity spikes in the conduction- and valence bands (see Fig. 2.7) [15]. These spikes can both create extra barriers for the electrons to overcome or tunnel through, and may also work as potential wells with discrete energy states [11]. The lattice mismatch causes dangling bonds at the interface (see Fig. 2.8). These dangling bonds become intermediate energy states, acting as recombination centers at the interface. They may also provide sites for quantum mechanical tunneling across the junction [11]. It is important to use semiconductors with very similar lattice structures, in order for the heterojunctions to have as near ideal properties as possible.

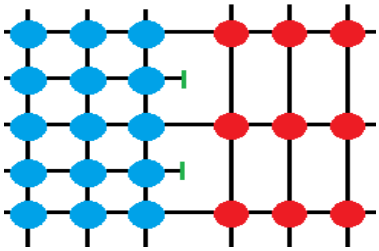

Figure 2.8: The mismatch between the lattices causes dangling bonds at the interface [15].

2.2.3 ZnO/Cu_2O heterojunction

An example of a heterojunction solar cell is a Cu_2O/ZnO cell, where the Cu_2O is spontaneously p-type and ZnO is n-type. The junction is supposed to work reasonably well because the conduction band edges of Cu_2O and ZnO align well, making the discontinuity spike seen in figure 2.7 small. Cu_2O is a good absorption layer material, and ZnO nanowires allow for good charge transport as well as high band gap and large interface, the latter allowing for thicker films and thus higher absorption [8]. Crystallographic orientation is important for achieving a good photoresponse from a p-Cu_2O/n-ZnO cell [9]. A ZnO/Cu_2O heterojunction cell deposited by electrodeposition has open circuit voltage 0.19V, short circuit current 2mA/cm, fill factor 0.295, and conversion efficiency 0.117% [10]. The conversion efficiency for a cell with Cu_2O deposited at optimum conditions (50%C with high pH) was 0.41% [7]. By rf-magnetron sputtering the above values were 0.26V, 2.8mA/cm^2, 0.55, and 0.4% respectively [9]. The efficiency is still very low. The introduction of an interface layer might improve the efficiency, but [8] report no success from using an interface layer of TiO_2. With ZnO being a good window layer, due to its high band gap and ease to form nanowires, combined with the Cu_2O being a good absorber and the good lattice match, the poor performance of these cells is disappointing.

2.3 Electrodeposition

This study mainly focuses on electrodeposition for deposition of oxides. Electrodeposition is a simple method for achieving high quality films at low temperatures and low production cost. In an electrodeposition process, ions are moved through a solution by an electric field to coat an electrode. The simplest form of an electrochemical cell is performed using a 2-electrode system, consisting of a cathode and an anode. In the 2-electrode system, the voltage is measured between these two electrodes, and the current is measured anywhere in the circuit. This system works very well under equilibrium conditions. However, if the electrochemical reactions taking place are not in equilibrium, the simple voltage measurement will be inaccurate due to red-ox potentials and overpotential [38]. To counter this problem a third electrode is introduced with the sole task of measuring the voltage on the working electrode versus a known, stable reference potential. This electrode is called a reference electrode. Different reference electrodes have different reduction potentials with a normalized hydrogen electrode (NHE) being defined as zero. The setup for this three-electrode system is shown in Fig. 2.9. The voltage is applied between the cathode and the anode. The cathode is the negative electrode and the anode is the positive electrode. In cathodic deposition the substrate is the cathode

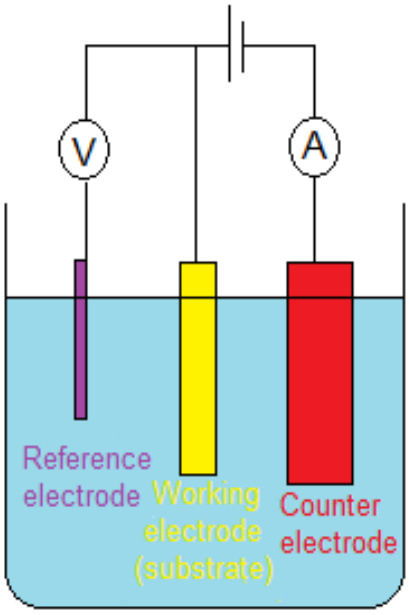

Figure 2.9: schematic of a 3-electrode setup.

and the counter electrode is the anode, and opposite for anodic deposition.

2.3.1 Working electrode

The working electrode is where the desired reaction should take place, and in the case of electrodeposition this electrode is also often the substrate. In electrochemistry the working electrode should have small area. It also should not chemically react with the test solution, and the surface should be smooth [38].

2.3.2 Counter electrode

The counter electrode supplies current to the reaction on the working electrode. In order to reduce the overpotential as much as possible, the electrode process should be oxidation or reduction of an electrolyte component to oxidation or reduction products. If possible it could be the opposite reaction of the working electrode, thus keeping the electrolyte composition constant [38].

2.3.3 Reference electrode

A good reference electrode should be at a constant potential independent of current density, which it will be if the reaction is reversible. Often used reference electrodes are NHE, SCE (saturated calomel electrode) and Ag/AgCl compared to using NHE and SCE the AgCl electrode has the advantage of being both environmentally friendly and easy to make. The different reference electrodes have different potentials, the NHE is defined as zero, and SCE and Ag/AgCl have potentials around

0.2V/NHE. The counter electrode may also act as reference electrode, though this setup gives less control over the applied potential due to overpotential [38]. According to [38], the counter electrode may work as reference for small currents.

2.4 The oxides

2.4.1 Zinc oxide

Zinc oxide is a direct band gap semiconductor/insulator with a 3.2eV band gap [14]. It is often used as a window layer in a heterojunction cell. The advantages of this material include being environmentally friendly, easy to deposit, and inexpensive. Zinc oxide thin films can easily be deposited by cathodic electrodeposition. In the case of ZnO electrodeposition from zinc nitrate, the test solution of $Zn(NO_3)_2$ creates Zn^{2+} and NO_3^- ions. Exactly how ZnO is deposited is unknown, but the following scheme has been suggested [4]:

$$Zn(NO_3)_2 \rightarrow Zn^{2+} + 2(NO_3)^- \tag{2.2}$$

At the cathode surface the pH is locally higher [17], perhaps due to the following reaction [4]

$$NO_3^- + H_2O + 2e^- \rightarrow NO_2^- + 2(OH)^- \tag{2.3}$$

The Zn^{2+} and the OH^- then combine to create $Zn(OH)_2$, and at lower temperatures the reaction stops here [17]

$$Zn^{2+} + 2(OH)^- \rightarrow Zn(OH)_2 \tag{2.4}$$

However, if the temperature is high enough, ZnO is the favored compound [17]:

$$Zn(OH)_2 \rightarrow ZnO + H_2O \tag{2.5}$$

The final equation for ZnO deposition becomes [17]

$$Zn^{2+} + NO_3^- + 2e^- \rightarrow ZnO + NO_2^- \tag{2.6}$$

Depending on whether one wants to produce a uniform film or a film consisting of nanorods one can apply different combinations of solutions. For a uniform film, a dilute solution of $Zn(NO_3)_2$ is all that is needed, along with a counter electrode of pure metallic Zn [3, 4]. Another method to achieve a smooth ZnO film mentioned in the literature, is applying an unspecified zinc salt along with dissolved oxygen as solution for electrodeposition [5, 17, 18]. For nanorods, the only requirement of the counter electrode is not to take part in the reaction, while the solution consists of $Zn(NO_3)_2$ and HMTA (hexamine). In the latter case it is not necessary to apply an external voltage if the solution is saturated or close to saturated. In the solution, Zn^{2+} ions create complexes with six water molecules [19], before they at the electrode surface combine with OH^- ions to perform the reaction [18]:

$$Zn^{2+} + 2OH^- \rightarrow ZnO + H_2O \tag{2.7}$$

The ideal applied voltage for electrodeposition of ZnO depends on the reference electrode and the electrolyte solution used. Different reference electrodes have different potentials. For different electrolytes there will be different reactions taking place. If the electrolyte consists of dissolved oxygen and a zinc salt, any potential between the reduction potentials of metallic Zn and ZnO during the deposition will cause ZnO to be deposited [5], while for a solution of $Zn(NO_3)_2$ one has to take into consideration the reduction of nitrate as well, the most efficient potential being between -0.7 V/SCE

and -0.88 V/SCE [20]. When depositing thin films, Izaki *et al.* found that the smoothest film was obtained with an applied potential of -1.0 V/Ag/AgCl [4]. Due to the reduction potential of metallic Zn being -0.76 V/NHE, for voltages more negative than -0.9 V/NHE, deposition of metallic zinc has occurred. And if it reaches -1.2 V/NHE more Zn will be deposited than ZnO, according to [6, 21]:

$$\mathrm{Zn^{2+}} + 2\mathrm{e^-} \rightarrow \mathrm{Zn} \qquad E_0 = -0.76\mathrm{V/NHE} \tag{2.8}$$

With the overall reaction for deposition of zinc oxide being [5]

$$\mathrm{Zn^{2+}} + \frac{1}{2}\mathrm{O_2} + 2\mathrm{e^-} \rightarrow \mathrm{ZnO} \qquad E_0 = 0.93\mathrm{V/NHE} \tag{2.9}$$

If the applied voltage is more negative than -1.2V/NHE metallic zinc will be deposited:

$$\mathrm{Zn(OH)_4^{2-}} + 2\mathrm{e^-} \rightarrow \mathrm{Zn(s)} + 4\mathrm{OH^-} \qquad E_0 = -1.20\mathrm{V/NHE[22]} \tag{2.10}$$

Hence if the applied potential is between 0.93 V/NHE and -0.76 V/NHE, ZnO will be deposited. If the applied voltage is more negative than -0.76 V/NHE, there might also be some metallic zinc deposited. -0.7V to -0.88V is the range in which the reduction of nitrate is most efficient, and therefore it is the best range for deposition of ZnO from a $\mathrm{Zn(NO_3)_2}$ solution [20]. Too large positive voltages will therefore result in no film deposition. The best voltage for electrodeposition of ZnO from $\mathrm{Zn(NO_3)_2}$ is reported to be approximately -0.9V vs. a reference electrode with reduction potential around +0.2 (SCE, Ag/AgCl) [3, 20, 21].

2.4.2 Copper oxide

Copper oxide can be either copper^{I}oxide or copper^{II}oxide. The two materials have different properties. $\mathrm{Cu_2O}$ has 2.05eV band gap, while the band gap for CuO is 1.2 eV [23]. $\mathrm{Cu_2O}$ is considered to be very promising for solar cells applications due to high absorption coefficient and low production cost [9].
For electrodeposition of copper oxide copper ions need to be freed, as by the following reactions[22]

$$\mathrm{Cu^{2+}} + \mathrm{e^-} \rightarrow \mathrm{Cu^+} \qquad E_0 = 0.16\mathrm{V/NHE} \tag{2.11}$$

$$\mathrm{Cu^{2+}} + 2\mathrm{e^-} \rightarrow \mathrm{Cu(s)} \qquad E_0 = 0.34\mathrm{V/NHE} \tag{2.12}$$

$$\mathrm{Cu^+} + \mathrm{e^-} \rightarrow \mathrm{Cu(s)} \qquad E_0 = 0.52\mathrm{V/NHE} \tag{2.13}$$

From these reactions it would seem that deposition can only be carried out at positive voltages, as negative voltages all would lead to deposition of metallic copper. However, as in deposition of zinc oxide, hydroxide makes deposition of metal oxide possible even at voltages at which otherwise deposition of pure metal would occur. Cathodic electrodeposition of $\mathrm{Cu_2O}$ is normally prepared from a buffered copper salt solution made from copper sulfate, lactic acid and sodium hydroxide, usually in high concentrations and with a high final pH [26, 27]. The applied potential is then normally 0.5V vs. a copper anode [23]. When depositing from an acetate solution co-deposition of copper and copper oxide occur at voltages more negative than -0.4V/SCE, but deposition of $\mathrm{Cu_2O}$ is achieved between 0 and -0.3V/SCE [24]. CuO is not normally made by electrodeposition directly, but rather by oxidation of $\mathrm{Cu_2O}$ [25].

2.4.3 Silver oxide

Silver oxide appears as Ag_2O and AgO. The latter is indeed believed to be $Ag^{I}Ag^{III}O_2$ [28]. Ag_2O is a p-type semiconductor of bandgap 1.3 ± 0.3eV [29].
AgO has 1.1eV band gap and has been electrodeposited by Breyfogle et al. [30]. In this process a silver acetate solution mixed with sodium acetate was used as test solution while a silver wire acted as reference electrode. Metallic silver deposition occurred at -0.07V vs this reference, and silver oxide was deposited at positive voltages (current density 0.25mA/cm2, or 2.5μA/mm2). Silver oxide deposition could follow the reactions below when in an alkaline solution:

$$2\mathrm{Ag(s)} + 2\mathrm{OH^-} \rightarrow \mathrm{Ag_2O} + \mathrm{H_2O} + 2\mathrm{e^-} \qquad E_0 = 0.34\mathrm{V/NHE[22]} \tag{2.14}$$

$$\mathrm{Ag_2O(s)} + 2\mathrm{OH^-} \rightarrow \mathrm{Ag_2O_2} + \mathrm{H_2O} + 2\mathrm{e^-} \qquad E_0 = 0.60\mathrm{V/NHE[22]} \tag{2.15}$$

Reaction 2.14 shows that for voltages higher than 0.34V/NHE deposition is of Ag_2O while it is Ag(s) being deposited otherwise. If the voltage is higher than 0.60V/NHE Ag_2O_2 is deposited, as seen from reaction 2.15. Deposition of silver oxides are more easily performed in alkaline solutions [29], or from nitrates (see Reaction 2.3). If no hydroxide is available the reaction is:

$$\mathrm{Ag^+} + \mathrm{e^-} \rightarrow \mathrm{Ag(s)} \qquad E_0 = 0.80\mathrm{V/NHE[22]} \tag{2.16}$$

Electrodeposition of AgO has been performed on stainless steel, polycrystalline platinum and ITO-covered glass [30]. Cathodic deposition from silver nitrate solution was performed by [31], and the resulting film consisted of silver particles a few μm across.

2.4.4 Silver copper oxide

Silver copper oxides are promising absorbers with calculated low direct band gaps and high absorption coefficients [32]. The first silver copper oxide, $Ag_2Cu_2O_3$, was produced in 1999 by Gomez-Romero et al. [35]. This material can be further oxidized into $Ag_2Cu_2O_4$, or $AgCuO_2$. According to calculations, $Ag_2Cu_2O_3$ is metallic in nature while $Ag_2Cu_2O_4$ is a low band gap semiconductor [32].
It has been suggested that $Ag_2Cu_2O_4$ has the same structure as AgO, which is $Ag^{I}Ag^{III}O_2$, where Cu^{III} occupies the places held by Ag^{III} due to Cu^{III} being the most stable[28]. However, [34] concludes the AgO structure is not a perfect reference for the structural and electronic properties of $Ag_2Cu_2O_4$, and that the assumptions in [33] are not all sound. Further, no valence splitting is found for silver in $Ag_2Cu_2O_4$ in [34].
Copper oxide can be deposited cathodically [23, 24] while silver oxide is deposited anodically [30, 29]. To make a film of silver copper oxide one could try depositing it as a copper oxide film containing silver or as a silver oxide film containing copper. Depositing these films by electrodeposition can be performed in a solution of silver and copper nitrates, possibly with increased pH, or in an alkaline buffer solution containing silver and copper ions. In order to deposit silver copper oxide based on a copper oxide structure a negative voltage would be applied, similar to the deposition of copper oxides, and hopefully silver occupies the metal(I) state sites. A silver copper oxide based on the silver oxide structure would on the other hand be deposited on a positive voltage, similar to the deposition of silver oxide with copper occupying the metal(III) sites.
Electrodeposition would be a cheap and easy method for producing thin films of silver copper oxide, if this is possible. No reports on electrodeposited silver copper oxide thin films have yet been found. The previous methods for producing a silver copper oxide have gone by different routes. The first powder of this material produced was made from a mixture of saturated silver and copper nitrates,

where the pH was increased by NaOH, the resulting solid was then oxidized and the final result was determined to be $Ag_2Cu_2O_3$[35]. From this, $Ag_2Cu_2O_4$ powder was produced by electrochemical synthesis, by applying a 0.46V voltage vs. a Pt wire quasi-reference in a solution containing $Ag_2Cu_2O_3$ and NaOH [36]. $AgCuO_2$ powder is also made by mixing nitrates in a high pH solution, though here a K_2SO_8 catalyst was also applied [28, 33]. RF sputtering resulted in a mixture of $AgCuO_2$ and $Ag_2Cu_2O_3$ [37].

3. Instruments

3.1 Thermal evaporator

In a thermal evaporation deposition system a material is evaporated by heating and then deposited on the substrate by condensation. The heating is performed by resistive heating as a large current is applied across the boat, basket or crucible holding the material to be deposited (see Fig. 3.1). The deposition is performed in vacuum, thus increasing the mean free path of the evaporated atoms, ensuring most of them reach the substrate. Not all materials deposit well on all substrates. For example gold does not adhere to glass. Therefore, when gold was deposited on glass, a thin adhesive layer of Cr was deposited under the gold.

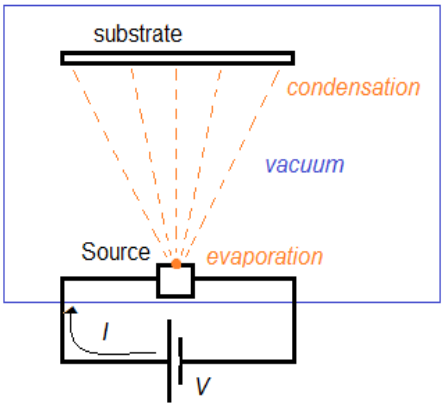

Figure 3.1: Schematic of thermal evaporation deposition.

3.2 Potentiostat

A potentiostat is an instrument that supplies a chosen voltage or current to a 3-electrode cell, and monitors the output current or voltage. In cyclic voltammetry, the supplied voltage oscillates between two different voltages at a constant scan rate. The current vs. voltage function is then plotted, showing rates of chemical deposition and stripping for the supplied voltages. Typical scan rates are 10-100mV/s. The potentiostat may also supply a constant voltage, constant current, and voltage or current step functions. For supplied voltage the current is plotted, and for supplied current the voltage is plotted. It is important that both of the other electrodes have electric contact with the working electrode. If there is no contact with the counter electrode, no current can be passed through, and if there is no contact with the reference electrode, the amplification circuit inside the potentiostat acts as an oscillator, causing wildly oscillating voltage supply.
A diagram of a typical potentiostat circuit is given in Fig. 3.2. A Pine Instruments WaveNow

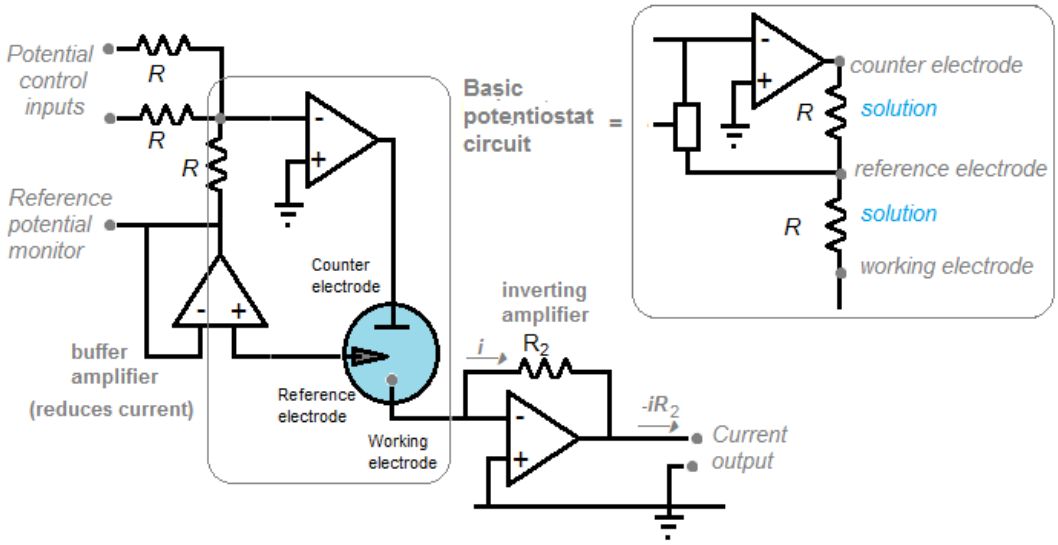

Figure 3.2: Circuit diagram of a typical potentiostat circuit[39].

potentiostat was used, which has a noise level of has 40nA [40]

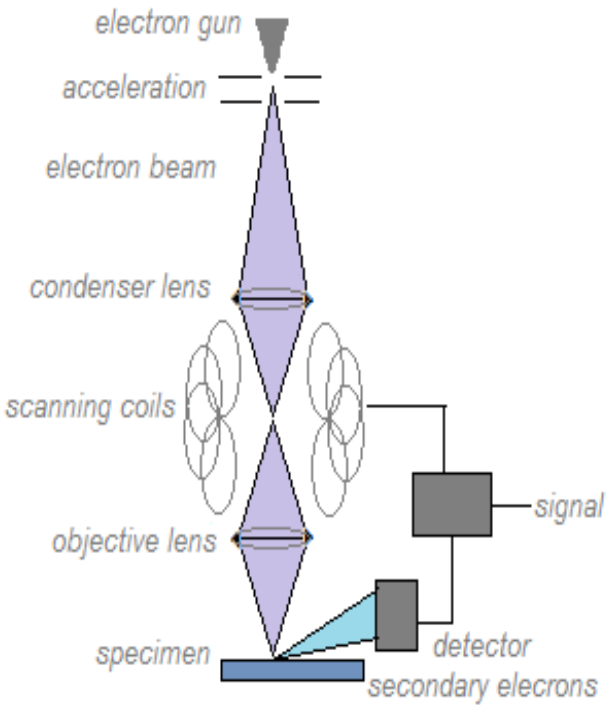

Figure 3.3: Illustration of a Scanning Electron Microscope.

3.3 SEM

A scanning electron microscope (SEM) is an instrument that directs an electron beam at the sample and collects the emitted secondary electrons to form an image. The secondary electrons are electrons that are re-emitted from the specimen, they form an image shows the topography of the sample surface in great detail. Backscattered (reflected) electrons can also be collected. The backscattered electron image shows topography and also composition. Backscattered electron intensity is dependent on the atomic number of the sample. The microscope consists of an electron gun, a condenser lens, scan coils, objective lens, the sample and an electron collector. The electron gun works by heating a filament slowly (to avoid fracturing) and accelerating the electrons using a voltage of 5-25kV. Electrons are collected and the intensity data is coupled with the scanning coils to create an image of the surface. The instrument works in a vacuum to increase the mean free path of the electrons in order for as many as possible to reach the appropriate detector [41]. A typical SEM is

shown in Fig. 3.3 In this work a JEOL JSM-S10 scanning microscope was used.

3.4 EDS/EDX

EDS/EDX stands for Energy-Dispersive X-ray Spectroscopy. The basic principle behind this technique is that different elements have unique electronic structures, and when bombarded with high-energy electrons they emit x-rays of characteristic energies. From this the elemental composition of the sample can be estimated.

3.4.1 Characteristic X-ray generation

Different elements have characteristic electron structures, and the core levels are not affected by the chemical environment of the atoms. The inner electron "shell" is called the K shell, the next is the L shell, then the M shell. An electron transition from one shell to the one below is labeled α, and a direct two shell transition is labeled β. A transition from the L shell to the K shell is thus labeled K_α. For these transitions to take place, the atom has to be excited. This happens (in the EDX) by an incident electron giving sufficient energy to one of the atom's lower shell electrons that it leaves the atom entirely. Then the atom, now an ion, goes to a lower energy state by filling this vacancy with an electron from a higher-energy shell. This transition is what emits the characteristic x-ray[42]

3.4.2 Difficulties

The electron beam loses energy further into the sample. This means that for atoms closer to the surface the incident beam electron energy is higher than deeper into the sample. Some energies are more likely to excite certain elements than others, and combined with the previous point it can be seen that the probability for excitation of an atom might either increase or decrease with depth. The x-rays also interact with the sample, and some are absorbed more easily than others, and therefore have a smaller probability of even reaching the detector. Any quantitative analysis will, due to these difficulties, be accurate only to within a few percent [42]. The tool is however useful for determining which elements are present in the sample and for mapping their distribution. The only difficulty of determining which elements are present is the fact that some lines may overlap.

3.5 XRD

X-ray diffraction is a technique used to determine the lattice parameter of a mono- or polycrystalline structure by reflecting x-rays off the surface and analyzing the diffraction pattern. The process in the x-ray source for emission of x-rays for x-ray diffraction is the same as the process for emitting characteristic x-rays in EDX. In order to create the diffraction pattern, the emitted x-rays must be of the same energy. This is achieved by bombarding a certain material (Cu and Mo are common materials) resulting in K_α radiation. These rays are further monochromatized by passing them through a filter or a single crystal. This monochromatic beam of x-rays then hits the sample, which reflects the radiation. The lattice structure of the sample, if there is one, then causes constructive interference in some directions [13]. This means the diffraction pattern will be mostly noise for amorphous structures, but for crystalline samples there will be a characteristic set of intensity peaks for the crystal orientations for each substance. The diffraction pattern is found by moving the detector around the sample while mapping the x-ray intensities, see Fig. 3.4. Typically, the x-ray source angle is called θ, and the detector angle is called 2θ.

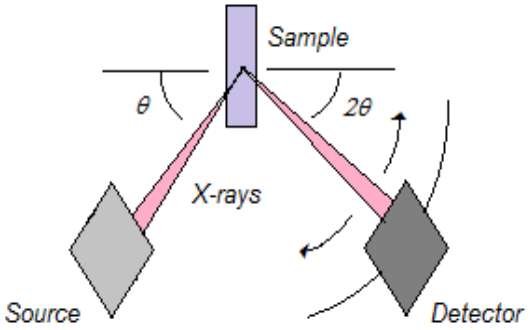

Figure 3.4: Illustration of the principles behind an XRD. The detector moves and registers the reflected intensity at different angles (2θ).

3.6 Optical measurements

Because the substrates were opaque, the optical properties of the films were found by measuring the reflecting light when the film was exposed to light of a certain energy spectrum. The returned spectrum then showed which wavelengths were absorbed and how much.

Because the source had a varying spatial content, and the detector had dark noise, a reference had to be chosen for reflectance measurements. The measured intensity I_M is given by:

$$I_M = I_{lamp} \cdot R_{sample} \cdot R_{substrate} + I_{dark} \tag{3.1}$$

Where I is intensity and R is reflectance. I_{lamp} is the intensity of the light source. The source was first calibrated with a spectrum showing the reflectance of the substrate. This was the "white" spectrum, where nothing was absorbed by the film. It was also calibrated to a "black" spectrum, I_{dark} where nothing was reflected. This was done by subtracting the dark spectrum from the measured spectrum, and dividing by the white spectrum:

$$R_{sample} = \frac{I_M - I_{dark}}{I_{lamp} \cdot R_{substrate}} \tag{3.2}$$

This gives the reflectance of the film directly, without having to correct for some of the light being absorbed by the substrate.

3.7 Thickness measurements

Thickness was measured with a Tencor Instruments alpha-step 100. The alpha-step measures a film's thickness by moving a needle along the sample surface. The vertical position of the needle is recorded as the needle moves, producing a graph of the topography of the film. When the needle

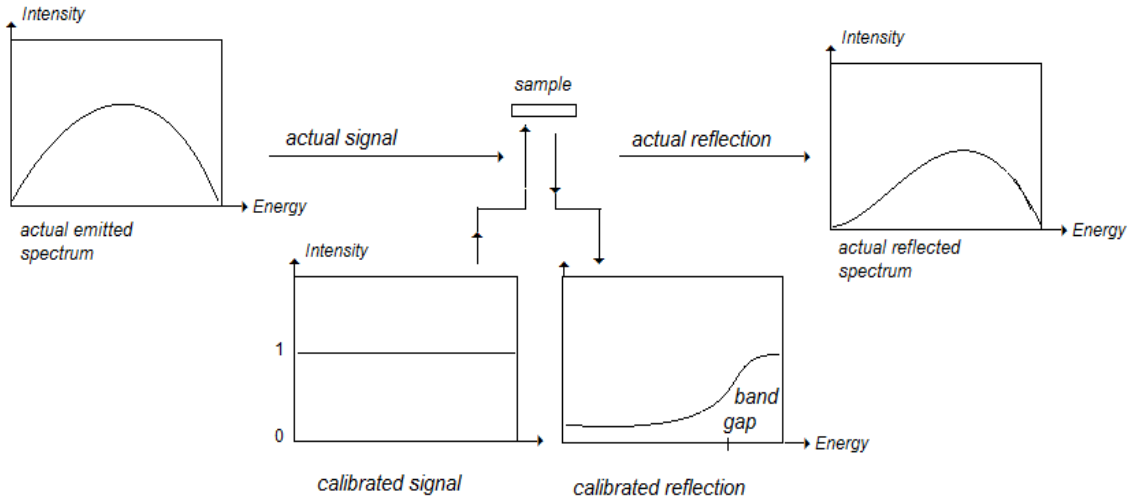

Figure 3.5: Illustration of the process of optical measurements.

passed from the substrate to the film, a sharp endge can be seen. The size of this edge is the thickness of the film.

4. Deposition

4.1 Substrate preparation

The substrates were microscope slides and Si wafers, and were cut into pieces 5 mm wide and 46mm long. Prior to each deposition the slides were cleaned in iso-propanol sonic bath for 5 minutes. They were stored in a container with iso-propanol until they were dried in a stream of nitrogen and placed in a vacuum chamber. Then a gold film approximately 3mm wide was deposited by vapor

deposition. First a thin layer (10Å) of chromium was deposited from a Cr-rod source at $2\cdot 10^{-5}$Torr, before a 1000Å thick gold film was deposited on top with the pressure slowly increasing to 10^{-4}Torr as the system heated. Typical deposition rates were 1-2 7Å/s for Cr, and 4-10 Å/s for gold. The gold was deposited from a Mo-boat source with a piece of 99.999% purity gold. For the samples with a ZnS interface layer this layer was deposited after the gold. The ZnS layer was deposited at $2\cdot 10^{-5}$ Torr and the layer was 14Å thick. The finished substrates were then placed in iso-propanol until electrodeposition was performed. Other substrates used were PtSi covered Si wafers cut into 4mm by 46mm pieces, similarly sized Cu foil and Al-foil and a tin rod. The Al foil was cleaned in acetone prior to deposition to remove production contaminants. The remaining substrates were rinsed in iso-propanol.

4.2 Electrodeposition

4.2.1 Setup

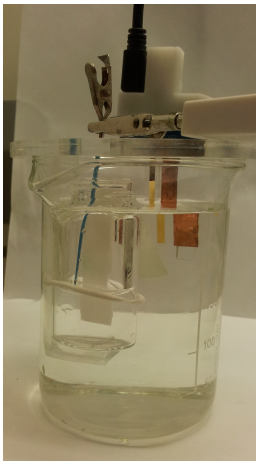

Figure 4.1: Photo of the 3-electrode setup with the reference electrode vial inside the test solution beaker connected by a salt bridge.

The electrodeposition setup consisted of a plexi-glass lid with holes for thermometer, pH-meter and the electrodes, with a special stand for the vial containing the reference electrode inside the beaker containing the electrolyte (see Fig. 4.1). This setup allowed the reference electrode to have the same temperature as the electrolyte and ensured equal distance between the instruments and electrodes for all depositions.

Reference electrode Depending on the material to be deposited, different reference electrodes were used:

- a Ag/AgCl in 3.0M KCl, connected by salt bridge to test solution was used for deposition of zinc oxide.

- copper or silver metal foil counter electrode was used when the test solution contained silver salts. Copper oxide was used for cathodic deposition and silver oxide was used for anodic deposition, as silver has a higher oxidation potential than copper.
- a separate silver metal foil electrode was used in experiments where the counter electrode would cause film deposition to avoid overpotential errors.

To test the reversibility of the reference electrode reaction, the reference electrode to be tested was made to act as working electrode in a 3-electrode setup, and cyclic voltammetry was run in order to get an overpotential vs. current plot. In a reversible reaction the curve would appear as a straight line with increasing and decreasing potential following the same path, while an irreversible reaction would give an elliptical curve, where the potential vs current curve is different if the potential is rising or falling [38].

This test proved the AgCl reference electrode to have a reversible reaction in KCl solution. The

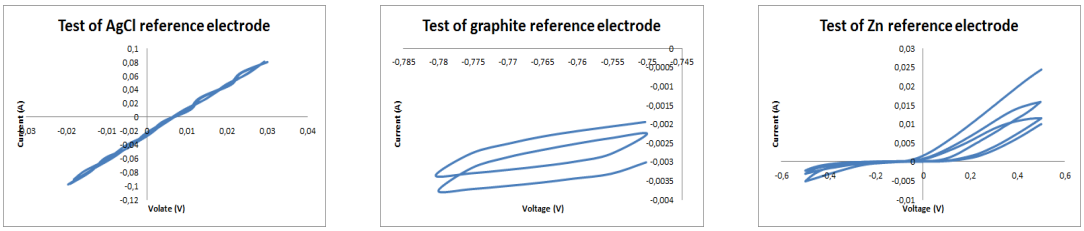

Figure 4.2: Cyclic voltammetry tests of reference electrodes AgCl in KCl, graphite in $Zn(NO_3)_2$, and Zn in $Zn(NO_3)_2$.

metal references were not entirely reversible, but the KCl solution could not be used in connection with silver nitrate solution, or precipitation of silver chloride would occur.

As the potential is not independent of chloride concentration and temperature, the reference electrode potential vs. working electrode was measured in order to get as accurate results as possible. The Ag/AgCl electrodes were cut out from a Pine Instruments Screen Printed Electrode and changed often. The contact between the reference electrode and the working electrode was measured prior to each deposition. The salt bridge was made by filter paper soaked in 3.0M KCl solution.

When depositions were performed in solutions containing silver nitrate, the counter electrode acted as the reference as well. Sometimes this led to significant deposition on the counter electrode, so a separate silver metal foil was also used as reference to avoid overpotential errors. This is believed to have the same small problem with reversibility as the Zn electrode in zinc nitrate solution (see Fig. 4.2), but the electrode behaves reproducibly and is stable, making it a sufficiently accurate voltage reference for this use.

Counter electrode For ZnO electrodeposition, Zn is a good choice, as it releases Zn^{2+} ions into the solution, thus keeping the electrolyte composition constant. Copper oxide was deposited with a copper counter electrode for the same reason. A silver counter electrode was used for silver oxide deposition. For the deposition of silver copper oxide, gold or platinum were considered as counter electrodes, because neither affects the electrolyte significantly. The problem presenting itself with this setup, and with the deposition of silver oxide, was the counter electrode having to work as reference electrode as well, due to Cl^- contamination from the 3-electrode setup. The gold counter electrode proved difficult to control as a reference. This problem can be remedied by two different

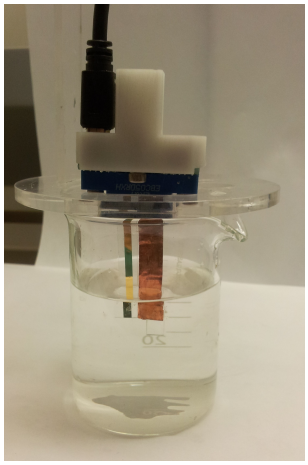

Figure 4.3: Photo of the 2-electrode setup with copper counter electrode and gold-coated substrate.

routes. One is to change the problematic material with a different one, e.g. for silver oxide deposition a silver counter electrode was applied, for copper oxide a copper counter electrode, and for silver copper oxide both materials were attempted. Another approach is the use of a copper or silver foil or wire as a reference electrode, and a counter electrode of the same material as the working electrode.

Working electrode The working electrode was also the substrate. Various materials were tried. The substrates used will be described in each section.

4.3 Electrodeposition procedure

Electrodepostition was performed differently for each oxide. First ZnO, then a short attempt at AgO and Cu_2O before the final attempt at electrodeposition of $AgCuO_2$. For ZnO cathodic electrodeposition was performed successfully. The other experiments had varying degrees of success.

4.3.1 Zinc oxide

Zinc oxide was deposited from a 0.1M zinc nitrate solution, prepared by dissolving 7.437g zinc nitrate hexahydrate in 250mL distilled water. The pH of this solution was found to be 5.13 at room temperature and 4.98 at 60°C.
Zinc oxide was deposited at 60°C, without stirring and with 60RPM stirring to avoid nanoflower crystals. The deposition voltages were -0.8V and -1.0V vs AgCl.

4.3.2 Copper and silver oxides

Copper and silver oxides deposition was attempted cathodically from their respective nitrate solutions. The copper and silver nitrate solutions both held concentration of 3.75mM, where the copper nitrate was prepared by dissolving 0.232g $Cu(NO_3)_2 \cdot 3H_2O$ in 200mL water, and the pH was measured to be 4.98. The silver nitrate was prepared by diluting 6.7mL 2.5% v/w silver nitrate solution

in 200mL distilled water. The pH in the silver nitrate solution was not measured because the reference electrode solution formed a white precipitate with the silver nitrate, likely silver chloride. Silver oxide deposition was also attempted anodically and cathodically from a solution containing 50mM silver lactate and 25mM sodium lactate. This solution was made by mixing 40.4945 g silver lactate salt, 28mL NaOH and 2.25mL 5% lactic acid and diluted to 50mL volume with distilled water. Cathodic voltages were -1.5V, -0.8V and -0.3V. Anodic voltages were 0.6V, 0.8V and 1V. However, no film was successfully deposited of silver oxide on any substrate except copper, which contaminated the film significantly. Cathodic deposition always gave visible metallic deposits.

4.3.3 Silver copper oxide

For the deposition of AgCuO2 100mL 5mM silver nitrate and 100mL 5mM copper nitrate was mixed. The concentrations were then 2.5mM, for each nitrate. The mixed nitrate solution was also combined in equal volumes (10mL each) with 45mM NaOH solution, resulting in a light green solution which slowly formed into "snowflakes" and settled in the bottom of the vial after approximately 40 minutes. This solution had pH 12. Higher concentrations led to faster precipitation. For these solutions stirring was applied after 20 minutes. Also a buffered solution containing a mixture of 0.1526 g silver lactate, 0.2497g copper sulfate, 0.75 mL 5% lactic acid and 10 mL 45mM NaOH solution was applied. Prior to the depositions cyclic voltammetry was performed in all solutions. The performed cyclic voltammetry experiments:

solution	voltage1	voltage2	scan rate
nitrates	0V	-1.5V	100mV/s
nitrates	1.2V	0V	25mV/s
nitrates+NaOH	1.2V	0V	25mV/s
silver lactate	1.2V	-0.3V	25mV/s
silver lactate +copper sulfate	1.2V/-0.2V	25mV/s	

The experimentation then followed the stages:

- Cathodic deposition at -1.5V, -0.8V, -0.3V and -0.15V vs. a copper counter electrode from pure nitrate solutions similar to the deposition of ZnO.
- Cathodic deposition at -0.8V vs. a copper counter electrode from pure nitrate solutions with stirring or heating.
- Cathodic deposition from nitrate mixed with NaOH.
- Anodic deposition on gold substrates and gold substrates covered with a 14Å layer of ZnS at various times and applied voltages (including oscillating voltages) of pure nitrate solutions.
- The step above with nitrate solutions mixed with NaOH.
- Anodic deposition of AgO on Cu_2O covered gold substrate.
- Anodic deposition on PtSi substrates at 0.9V applied voltage from nitrate solutions mixed with NaOH.
- Anodic deposition on copper substrate at 0.5V/Ag applied voltage from silver lactate/sodium lactate solution.

- Anodic and cathodic depositions from silver lactate/sodium lactate mixed with copper sulfate on gold and PtSi substrate.

Films were deposited from the cathodic deposition in pure nitrates and lactate mix, oscillating voltages, anodic deposition of alkaline nitrate solution on PtSi substrates and AgO deposition on Cu substrate. The experiments that yielded films:

solution	voltage/ counter electrode	substrate	time	other	result
nitrates	-0.15V/Cu	gold	20min	none	black film, metal
nitrates	-0.3V/Cu	gold	20min	none	black film, metal
nitrates	-0.8V/Cu	gold	20min	none	black film, metal
nitrates	-1.5V/Cu	gold	20min	none	black film, metal
nitrates	-0.8V/Cu	gold	20min	stirring	black film, large grains
nitrates	-0.8V/Cu	gold	20min	50C	black film, large grains
nitrates	-0.8V/Cu	gold	20min	80C	black film, large grains
nitrates+NaOH	0.9V/Ag	PtSi	20min	none	$Ag_2Cu_2O_4$
nitrates+NaOH	0.9V/Ag	PtSi	40min	none	$Ag_2Cu_2O_4$
nitrates+NaOH	0.9V/Ag	PtSi	180min	stir after 30min	$Ag_2Cu_2O_4$

Room temperature is 20°C. Experiments were carried out twice to test reproducibility. Chemicals were from Sigma-Aldrich except where noted otherwise. The pH meter was a HANNA Instruments HI991001 pH meter. The pH-meter's reference electrode likely contained a chloride solution. this solution reacted with the silver nitrate to form silver chloride. The pH-measurement is therefore a little inaccurate. I believe the NaOH concentration in the solution containing NaOH was a bigger influence on the pH than the (small) change in Ag^+ concentration due to the pH-meter. The measurement was performed quicky in order to minimize the inaccuracies. A more accurate pH could have been measured with pH paper. Heating and stirring were performed on a hotplate with a magnetic stirrer.

5. Results

Contents:

- **Cyclic voltammetry:** Deposition voltages are found.
- **Electrodeposition:** Description of the currents, depositions, and the resulting films.
- **Characterization:** SEM, EDS, XRD and optical measurements for all materials in turn.

5.1 Cyclic voltammetry

Cyclic voltammetry was used to determine promising voltages for deposition. The plots show voltages where depositions take place as increased current. The plots may also show voltages where stripping of an existing film takes place, as large current peaks with abrupt endings indicate there being no more material to strip. Different peaks sometimes correspond to depositions of different compounds, such as Cu_2O or metallic Cu. A peak shows the highest deposition rate for each material. A good deposition voltage should be in the voltage range of the desired deposition, without any other compound being deposited, and with a measurable current.

5.1.1 Zinc oxide

Cyclic voltammetry in zinc oxide, as seen in Fig.5.1, showed peaks at -0.7V vs AgCl and a big peak below -1.0V vs AgCl where metallic zinc was deposited. The large positive peak at -0.7V is likely due to stripping of the metallic zinc from the electrode. The voltage should therefore stay positive

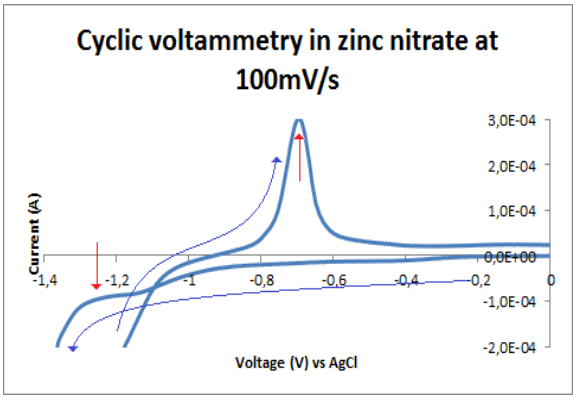

Figure 5.1: Plot of voltammetry run in 0.1M $Zn(NO_3)_2$ solution with 100mV/s scan rate. The red arrows point to the peaks, the blue arrows indicate the scan direction.

of -1.0V at all times or there will be metallic zinc deposited along with zinc oxide. Zinc oxide seems to be deposited at all negative voltages positive of -1.0V, but with particularly favorable growth at -0.8V.

5.1.2 Negative voltages in silver and copper nitrates

Cyclic voltammetry for negative voltages on gold substrate in silver nitrate yielded 2-3 peaks (see Fig. 5.2). Those were at -0.25V, -0.9V and somewhere below -1.5V, where likely metallic silver is deposited. Based on the cyclic voltammetry plot, the peaks visible could correspond to deposition of silver oxide, silver oxide mixed with metallic silver, and pure metallic silver. Based on the deposition of ZnO from nitrate, some co-deposition could be possible, especially in light of the multitude of peaks, despite the noble nature of silver.
Copper nitrate cyclic voltammetry, seen in Fig. 5.2, shows peaks at -0.5V and somewhere negative of -1.5V. The latter most likely represents the deposition of metallic copper, while the -0.5V/Cu peak is the highest deposition rate for a copper oxide, most likely Cu_2O. Cyclic voltammetry in the mix

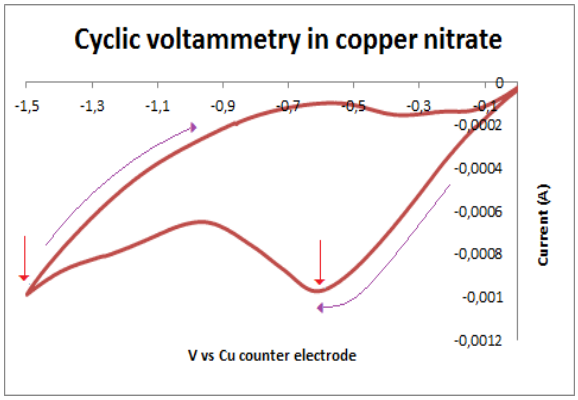

a)

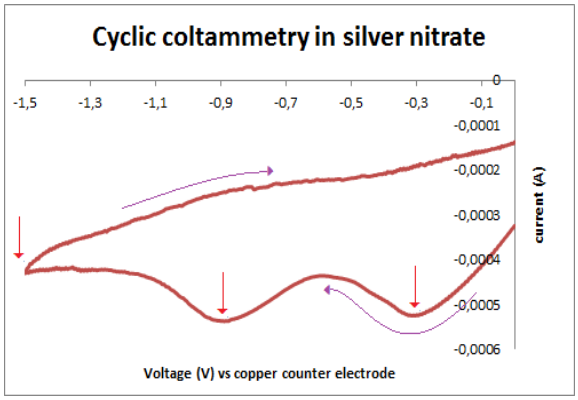

b)

Figure 5.2: Cyclic voltammetry plots for voltammetries performed in a) 3.75mM copper nitrate and b) 3.75mM silver nitrate. All voltages are vs the copper counter electrode. The red arrows point to the peaks, the blue arrows indicate the scan direction.

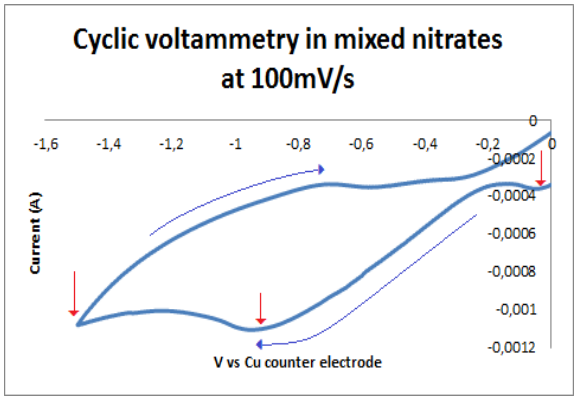

Figure 5.3: Plot of voltammetry run in a mixed 2.5mM silver nitrate 2.5mM copper nitrate solution with 100mV/s scan rate, the voltage is vs a copper counter electrode. The red arrows point to the peaks, whereas the blue arrows indicate the scan direction.

of silver and copper nitrates has three peaks (see Fig. 5.3). The first peak appear just negative of 0V. The next two peaks are at -1.0V and somewhere negative of -1.5V. These peaks may correspond to deposition of silver copper oxide or a mixture of silver oxide and copper oxide, co-deposition of silver and copper metals and their oxides, or a pure metal mixture. Based on this, the deposition voltages -0.15V, -0.3V, -0.8V and -1.5V (vs Cu) were chosen.

5.1.3 Positive voltages in mixed silver and copper nitrate

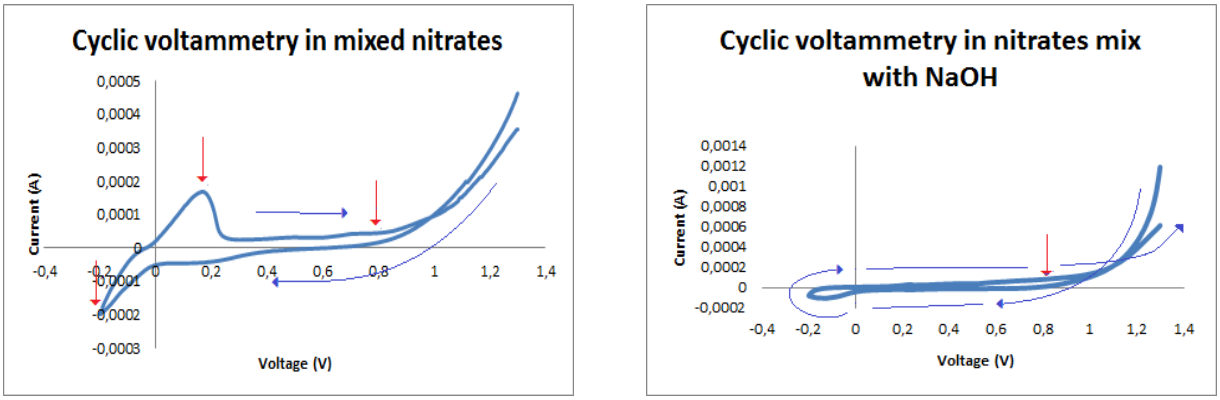

a) b)

Figure 5.4: a) Cyclic voltammetry of a solution with mixed silver nitrate and copper nitrate. b) The same solution mixed with NaOH, at 25mV/s scan rate. The voltages are measured against a silver metal counter electrode. The red arrows point to the peaks, whereas the blue arrows indicate the scan direction.

The positive voltage scans vs silver counter electrode (see Fig. 5.4) shows both the mixed nitrates with NaOH and the mix without start depositing anodically at 0.8V, with a steep increase continuing all the way to the end of the scan at 1.3V. After the scans the gold film was visibly loose, so 0.9V was chosen as deposition voltage in the hopes of keeping the gold attached. Also low voltage means low current density, which reduces overpotential error from using the counter electrode as voltage reference. It can also be seen that the solution containing NaOH does not have the same response to negative voltages as the one without. This is also beneficial when using the counter electrode as reference, as there is less danger of getting errors from depositions on the counter electrode. Once the voltage reaches above 0V again for the pure nitrates mix, there is a current peak from stripping of the working electrode. Anodic deposition from mixed nitrates should be performed in a solution mixed with NaOH at 0.9V vs. silver counter electrode. This voltage turned out to also strip gold from the substrate, the experiment was later performed on a PtSi substrate successfully.

5.1.4 Positive voltages in silver lactate

Cyclic voltammetry in a silver lactate sodium lactate solution showed a graph similar to the one reported in [30] (see Fig. 5.5). The voltammetry begins at the highest voltage, with deposition current. This deposition current is reduced until being zero at 0.6V/Ag. From there there is no current until the negative potentials, here deposition current appears as soon as the voltage is

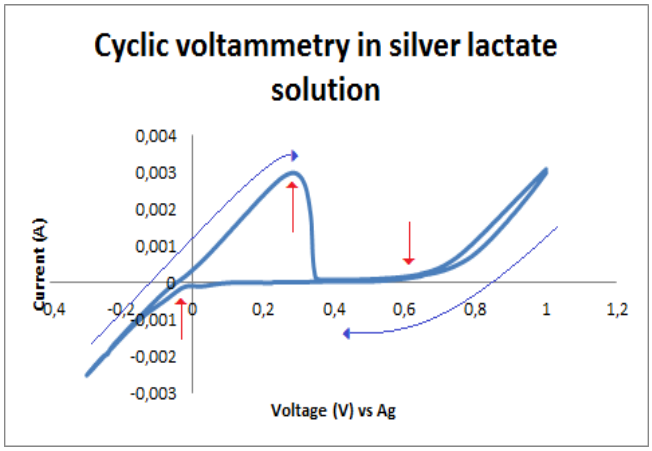

Figure 5.5: Cyclic voltammetry of a silver lactate sodium lactate solution. The red arrows point to the peaks, and the blue arrows indicate the scan direction.

negative. When the potential once again is positive, the current continues upward while stripping off the newly deposited layer. At 0.4V/Ag this stripping abruptly ends, and the current is flat until 0.6V/Ag, where it again increases due to deposition in the same track as before. Based on this, good deposition voltages should be anything positive of 0.6V/Ag.

5.2 Electrodeposition overview

Zinc oxide Electrodeposition of zinc oxide at both the applied voltages showed a current curve that increased at first, then decreased before it slowly flattened out. This happened because the layer of ZnO deposition on top of the gold is less conductive than the gold, so fewer electrons pass through. After a while the current flattens out because the gold is completely covered, and further deposition is ZnO on ZnO. The resulting films where white, non-transparent and brittle. A light microscope image of a ZnO film deposited at -1.0V/AgCl is shown in Fig. 5.7d). The deposition process likely happened as shown in Fig 5.6a), with the zinc bonding with the gold.
The thickness of a zinc oxide film deposited at -1.0V/AgCl was found to be greater than 25 microns by alpha-step.

Nitrates For cathodic deposition in solutions of silver nitrate, copper nitrate and a mix of the two, the current would sharply decrease and then flatten out during the first minute as the gold rapidly became covered in more insulating material. When in copper containing solutions a dark film would then have formed on the gold substrate. The current then stayed constant throughout the deposition, resulting in black films from solutions containing copper, and a milky film from the silver nitrate solution. When the temperature was increased or stirring applied the start of the deposition was the same, but the current then increased due to increasing roughness causing increasing surface area. These films were also thick and black, but the film had grown outside the

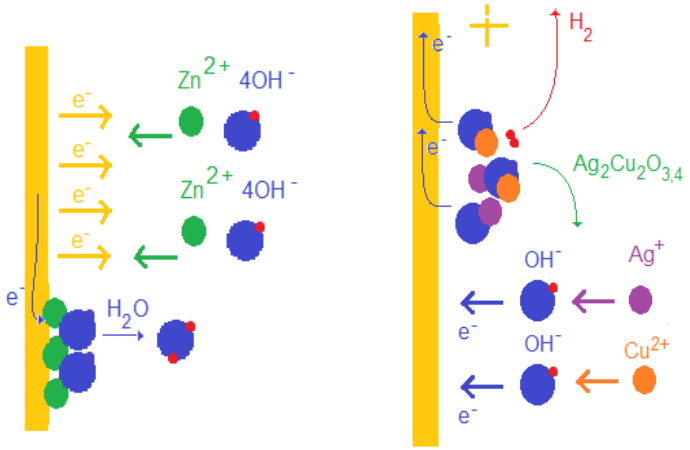

a) b)

Figure 5.6: a) Illustration of how zinc oxide is formed on a gold substrate by the gold and zinc bonding. b) Illustration of how the gold electrode acts as a catalyst, but not as a substrate. The oxygen is unable to bond with the gold, and the newly formed silver copper oxide (or silver oxide) precipitates rather than forming a film.

gold film on the microscope slide, and also covered much of the glass. This increasing area also occurred with deposition at room temperature without stirring for the -1.5V/Cu deposition. The increasing area suggests a highly conductive layer, probably silver and/or copper metal. Cathodic deposition from silver and copper nitrates probably happened in a process similar to Fig. 5.6a), though with silver no oxide was deposited. No film was obtained cathodically with NaOH in the mixture. From sliver lactate, cathodic deposition yielded film with a visible metallic sheen. The copper oxide film deposited at -0.3V/Cu was fuchsia and semi-transparent, while the -0.8V/Cu film was dark brown/black. These are shown in Fig. 5.7 e) and f), though much of the microscope light was absorbed, so the films appeared darker than they did to the naked eye. Anodically, no films were deposited on the gold substrate. This is likely because of the gold does not bond well with oxygen. The gold electrode therefore acted as a catalyst, but not as a substrate for deposition, see figure 5.6b). At high voltages (approximately 0.7V/Ag or more) the gold would also come free of the glass substrate, making deposition impossible. This probably was a result of the high voltages causing the adhesive Cr layer to dissolve, leaving the gold unattached to the glass.
On different substrates this should be remedied. For the deposition of silver copper oxide PtSi proved to be sufficiently conductive and reactive for a film to form on the surface at 0.9V vs a silver counter electrode. The current started high, around 100μA, but quickly decreased to only a few μA, which is an indication of a low deposition rate. The resulting film had a smooth, pale grey appearance, with some rust colored spots (see Fig. 5.7a)). Large areas of the film were smooth, though, like in Fig. 5.7b)). The spots may be silver oxide, copper oxide or simply a thicker layer of silver copper oxide. For silver oxide, which should be possible to deposit from silver lactate solution [30], only a copper substrate yielded a film. This film had a porous green appearance when wet, and slowly

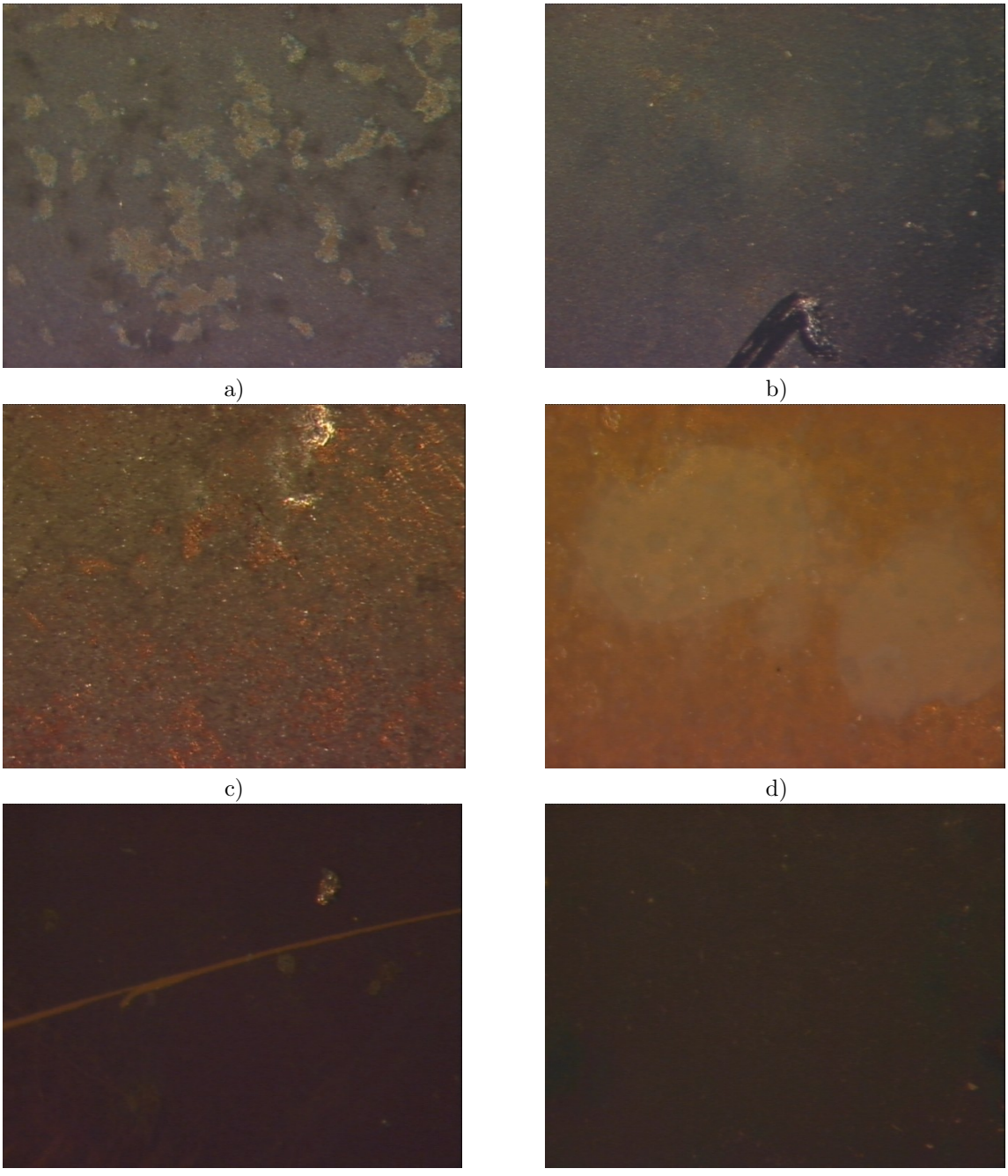

Figure 5.7: Light microscope images of a) spots on the surface of the silver copper oxide film. b) The film also consisted of large smooth areas. The scratch demonstrates the uniformity of the deposit, and a collection of material can be seen near the end. c) The film deposited from silver lactate on a copper substrate. d) Zinc oxide film deposited at -1.0V/AgCl. e) Copper oxide film deposited at -0.3V/Cu from copper nitrate solution. f) Copper oxide film deposited at -0.8V/Cu from copper nitrate solution.

dried to a grey-ish green color. The green wet film looked much like the solution after mixing silver and copper nitrates with NaOH, and therefore likely is some sort of silver/copper oxide/hydroxide mix. Much copper was freed into the test solution during this deposition, as a thick black film, like the cathodically deposited copper containing films, formed on the counter electrode.

5.3 Zinc oxide films

5.3.1 SEM

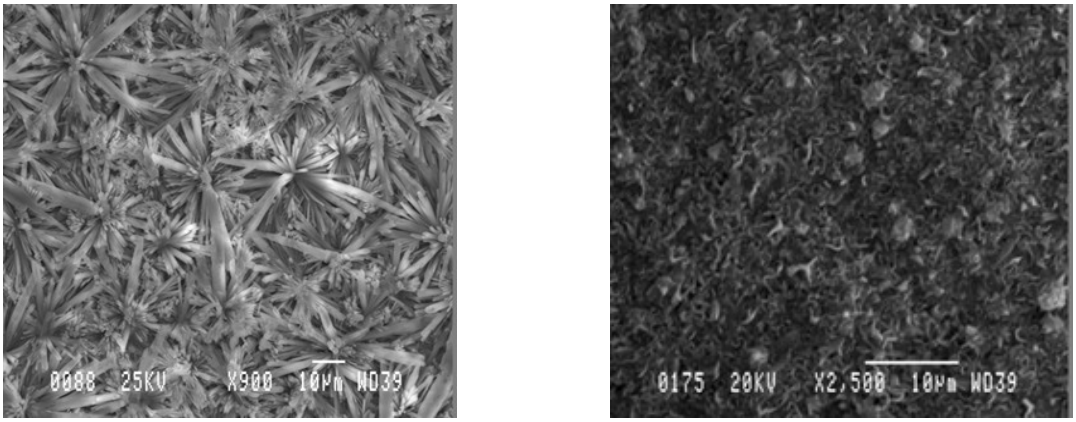

a) b)

Figure 5.8: a) ZnO film deposited at -0.8V/AgCl without stirring. b) ZnO film deposited at -0.8V/AgCl without stirring.

Depositions performed without stirring had obvious nanoflower structure over large parts of the films (see Fig. 5.8a)). This is probably due to the growth nucleating from certain points in the substrate. The films deposited with stirring were smooth but brittle (see Fig 5.8b)). Large cracks and flaking can be observed (see Fig. 5.9a)).
The surface itself seems to be a mixture of half formed spherical crystals and a rough-looking surface without any well-defined structure. Deposition at a more negative voltage increases the size of the roughly spherical structures, but otherwise looks the same (see Fig. 5.9). There is some reduction of cracks when the voltage is -1.0V/AgCl. The film thickness also increases with higher voltage.

5.3.2 XRD

XRD of the zinc oxide film shows plenty of characteristic peaks for various crystal orientations. The results point towards a polycrystalline film (see Fig. 5.10).

5.3.3 Optical measurements

The zinc oxide film reflected less than 4% of the light across the whole spectrum. Likely the film scattered much of the light, as its visual appearance was white. There is however a defined edge at 3.2-3.5eV. For shorter wavelengths no light is reflected, and for longer wavelengths 2-4% of the light

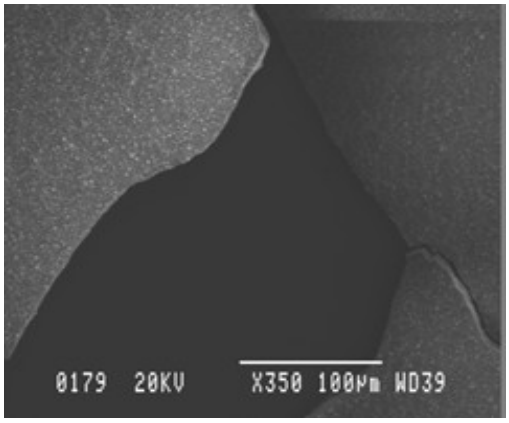

a)

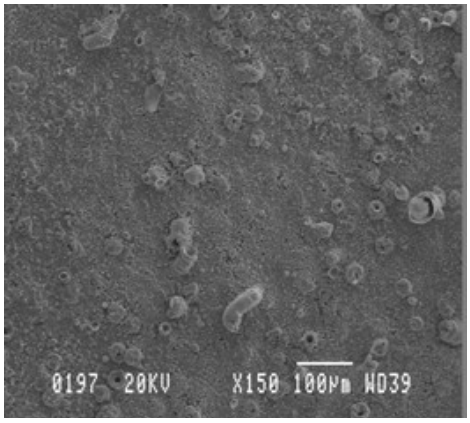

b)

Figure 5.9: a) Cracks in a ZnO film deposited at -0.8V/AgCl with stirring. b) SEM image of ZnO film deposited at -1.0V/AgCl with stirring.

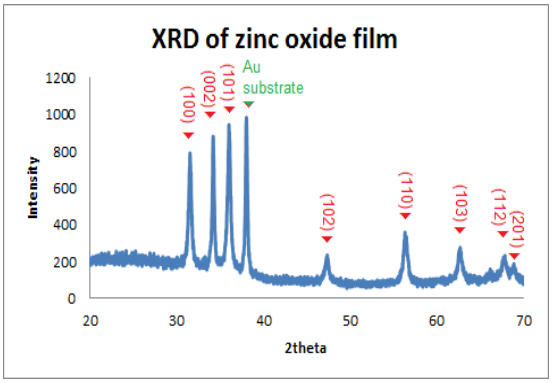

a)

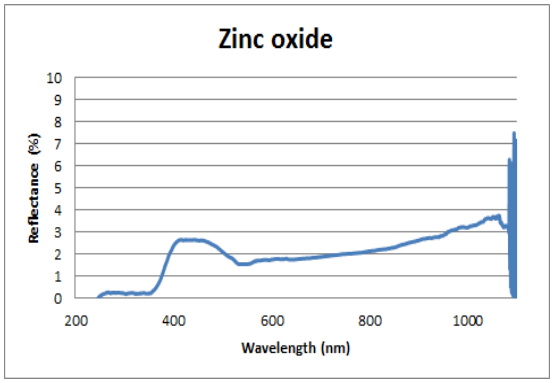

b)

Figure 5.10: a) X-ray diffraction of zinc oxide film deposited at -0.8V vs AgCl for 20 minutes. The peaks are identified from [43]. b) Reflectance of a zinc oxide film deposited at -0.8V vs AgCl

is reflected. 3.2-3.5eV is a reasonably good match to published values for the ZnO band gap. The Reflectance plot is shown in Fig. 5.10b).

5.4 Silver oxide

Despite many attempts, silver oxide was not successfully deposited by anodic deposition as reported in [30]. The procedure did not yield any films on any substrates other than copper, which likely contaminated the film.

5.4.1 SEM

The film on the copper substrate appears as large crystals on the substrate. In EDS mapping, it can be seen that the large crystals are made of silver with a shadow of oxygen. The copper has opposite distribution, being the substrate, though some copper can be seen even in the silver containing parts. This suggests that the copper is found in or near the substrate with a layer of silver oxide crystals on top. The oxygen seems to be bound to the silver for the most part. It might be the metallic copper substrate is all the copper measured, but the greenish appearance of the film suggests otherwise. This would mean there is copper oxide mixed in the silver oxide, though the silver oxide is most prominent.

5.4.2 XRD

The silver oxide on copper substrate film has a large peak from copper [27]. The remaining peaks correspond to Ag_2O_2 [30], CuO [25] and Cu_2O[24, 27]. This indicates the film is mostly a mixture of silver oxide and copper oxide. There are no peaks corresponding to $Ag_2Cu_2O_4$ or $Ag_2Cu_2O_3$. The film does in other words appear to be made out of a polycrystalline mix of metal oxides rather than a mixed metal oxide. The deposition process likely involved copper oxide being deposited from the inside, with hydroxide reacting with the copper on and immediately near the substrate. Silver would be deposited from the outside, with silver ions following the hydroxide towards the substrate. This is in accordance with the map from the EDS. The XRD plot is shown in Fig. 5.11e).

5.4.3 Optical measurements

The film deposited as silver oxide/copper oxide on a copper substrate from silver lactate solution shows a some resemblance to the $Ag_2Cu_2O_4$ film for wavelengths greater than 600nm. For the shorter wavelengths there seems to be much reflectance, indicating green or blue color. This was also seen on the film. This is possibly because of CuO, as the same behavior was later seen from the film deposited at -0.3V/Cu from a copper nitrate solution. The plot of the reflectance is shown in Fig 5.11f).

5.5 Cathodic deposition of silver and copper compounds

Cathodic deposition from silver nitrate, copper nitrate and a mixture of the two.

5.5.1 SEM and EDS/EDX of films deposited at -0.8V/Cu

It appeared from the current densities during deposition that -0.8V/Cu was the deposition voltage with the most equal amounts of silver and copper deposited, as the density at this voltage was the same for both copper and silver nitrate. SEM imaging shows the film deposited from copper nitrate to be very smooth (see Fig. 5.12b), so that very high magnification was needed in order to see any structures on the surface. The film deposited from silver nitrate has the same appearance as the silver particle films found in [31], and are likely metallic silver (see Fig. 5.12a)). The silver copper oxide attempt was hoped to mix silver and copper in the silver copper oxide. The appearance from the SEM is however that the silver agglomerates to form islands in the copper oxide film, as seen in Fig. 5.13.

This is confirmed by EDX mapping of the film shown in Figure 5.14. Here it can be seen that the silver is clustered in a coral-like structure, while the copper and oxygen is relatively evenly distributed

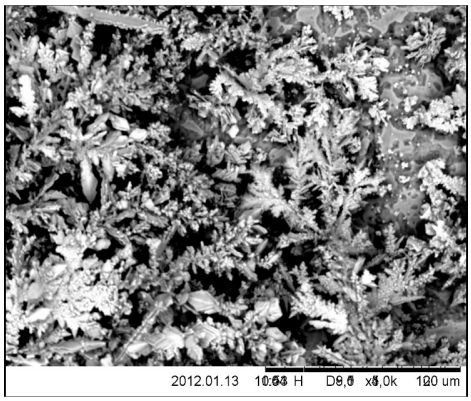

a)

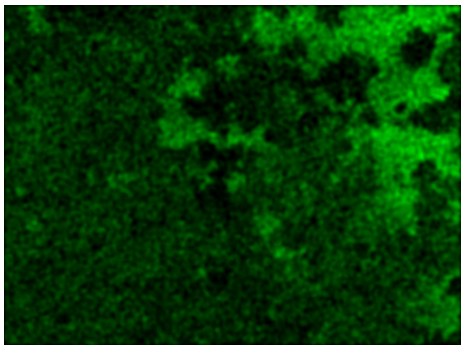

b)

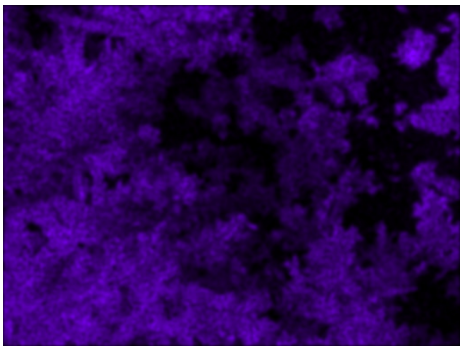

c)

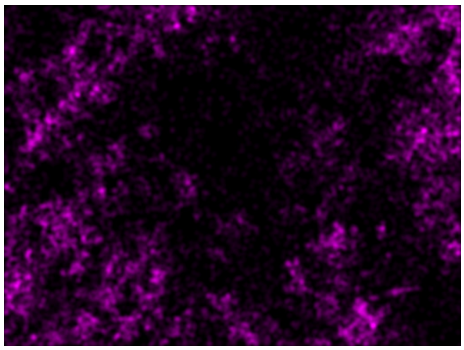

d)

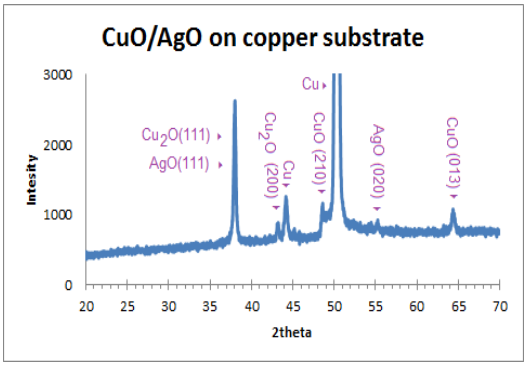

e)

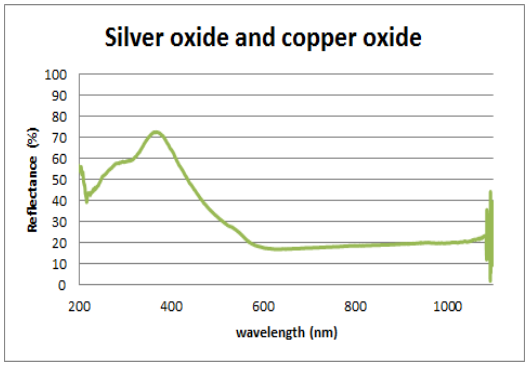

f)

Figure 5.11: The film deposited on a copper substrate in silver lactate in a SEM image (a), with a map of copper (b), silver(c) and oxygen (d) distribution in the same area. e) X-ray diffraction of film deposited as Ag_2O_2 on Cu substrate. The peaks are found from [24, 25, 27, 30]. f) Reflectance of the silver oxide/copper oxide film deposited on a copper substrate from silver lactate solution.

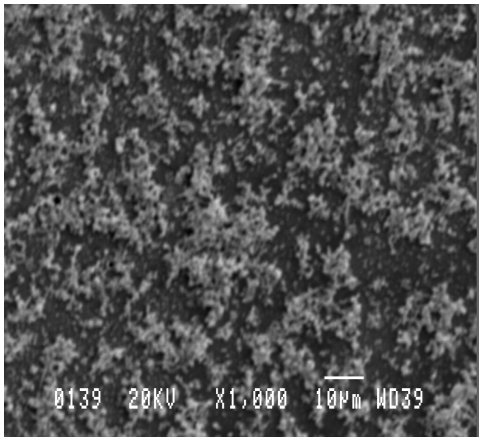

a)

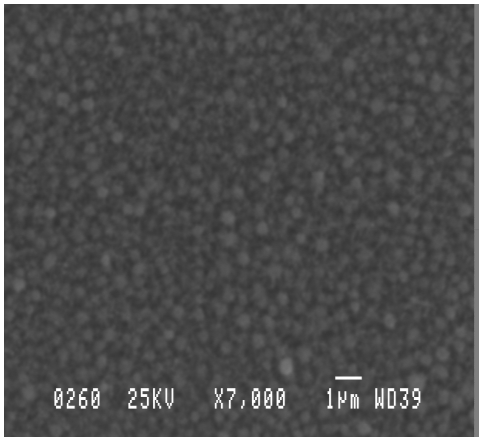

b)

Figure 5.12: SEM images of films deposited from silver nitrate (a), copper nitrate (b), deposited at -0.8V. Note that the images have different magnification

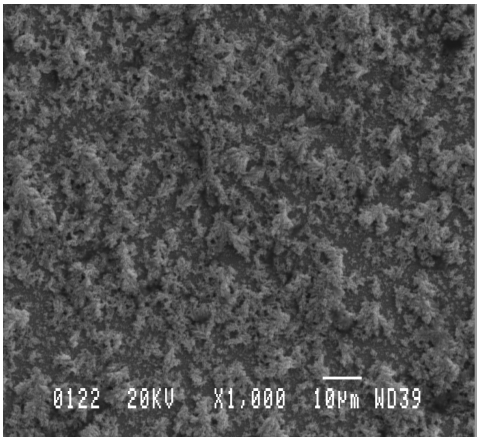

Figure 5.13: SEM image of a film deposited at -0.8V/Cu from a solution of silver nitrate and copper nitrate.

across the rest of the image. Deposition from the nitrate mix at -0.8V was also carried out with stirring and at elevated temperatures in the hopes that this would force the silver to mix better with the copper to achieve smoother films. What was indeed achieved was large crystals formation and an uneven surface. It appears that with higher mobility in the solution, larger clusters are formed, see Figure 5.15(a)-(d). The films deposited at room temperature without stirring were mostly smooth but with small clusters of silver. With higher temperature the surface seemed more porous, and structures started to form. With stirring a smooth surface with scattered lumps of material was achieved.

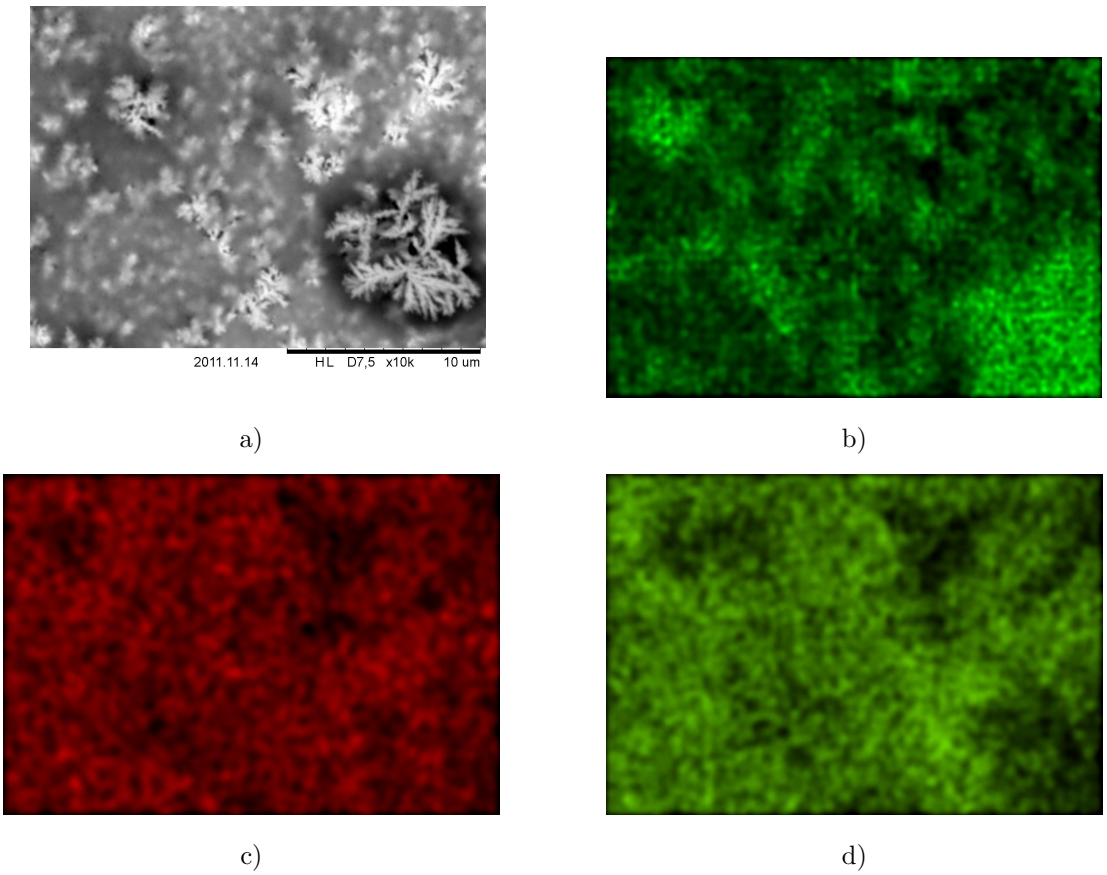

Figure 5.14: Elements distribution in the film deposited at -0.8V. a) SEM image, b) silver map, c) copper map, and d) oxygen map.

5.5.2 SEM and EDS of mixed compounds deposited at -0.3V/Cu and -0.15V/Cu

For smaller voltages (-0.3V and -0.15V vs Cu), which are common voltages for deposition of copper oxide in the literature, these lumps are smaller, and the silver seems to be distributed more evenly across the sample (see Figure 5.16). It remains to be seen if this silver is oxide or metallic in nature. This can be seen in XRD, as the peaks either correspond to metallic silver or a silver oxide. The images suggest that there are lumps of metallic silver, but perhaps some silver oxide is mixed into the copper as well. The deposition rate of silver/silver oxide is higher than the deposition rate of copper oxide at -0.3V/Cu, which leads to different concentrations, as seen in the quantitative analysis is in Figure 5.17. The analysis is sufficiently accurate for measuring the relative amounts of silver and copper, the comparison with the other elements (like oxygen) have too much error for reliable results. The film deposited at -1.5V was as expected found to be a mixture of metals deposited unevenly onto the substrate.

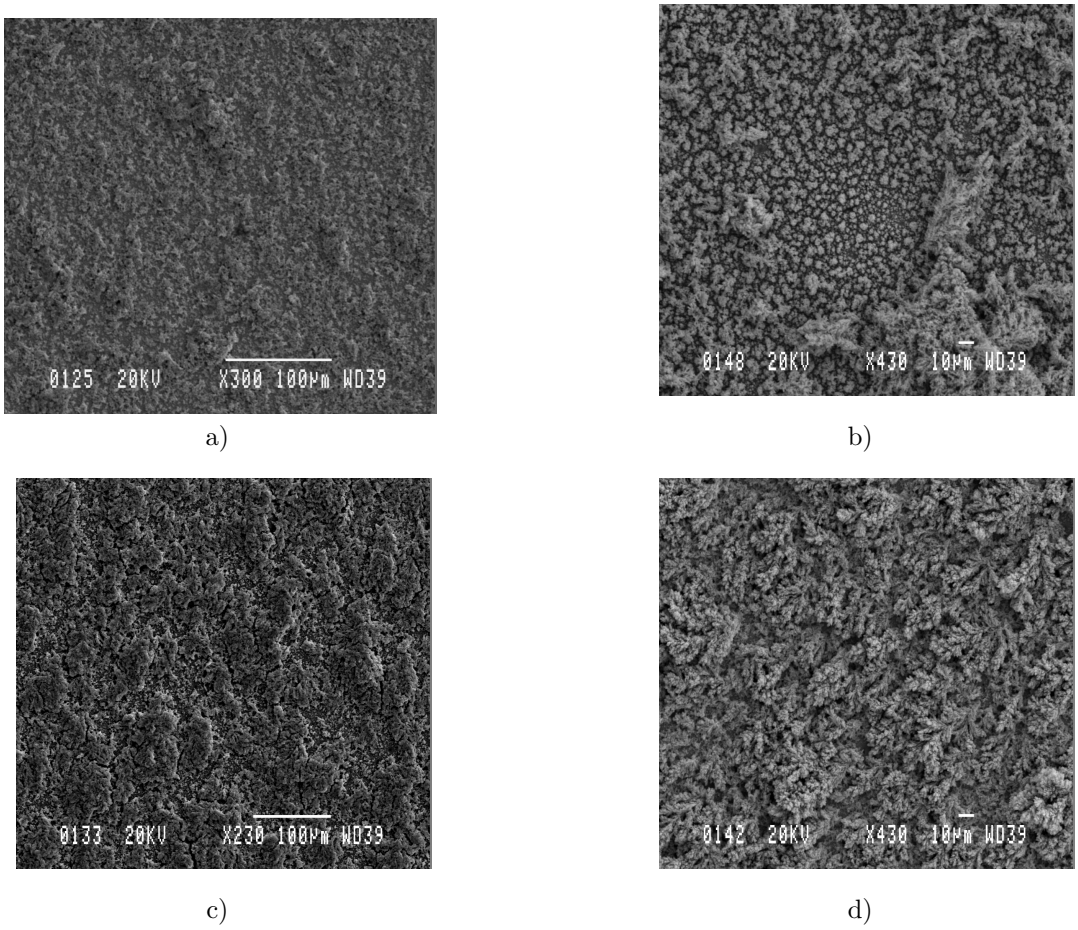

a) b)

c) d)

Figure 5.15: SEM images of films deposited from mixed nitrate solution at -0.8V at room temperature without stirring (a), with 80rpm stirring (b), 50°C (c), 80°C (d).

5.5.3 XRD of films from mixed nitrates

The films deposited at -0.8V both had mostly amorphous characteristics, except for the prominent peak from the substrate (see Figure 5.18b)). There might be a very noisy peak between 30 and 40 degrees, likely corresponding to the silver metal (200) peak marked in Fig. 5.18a). The film deposited at -0.15V however, showed a side-peak corresponding to Cu_2O deposited at low voltages [24] and a smaller peak corresponding to the (200) peak for silver metal [31], see Figure 5.18a). There were no peaks that could be due to silver oxide. A big peak from the substrate could also be seen. This means the silver seen in EDS was indeed metallic, and not oxide, for both the films. It also tells that the films grown at the smaller voltage had a more clearly defined crystal structure than the films grown at higher voltage. This is probably because films grown at smaller voltages grow slower, causing bigger crystals. The silver is also spread out more, as seen in the EDS maps. If the silver grown at higher voltages have a more amorphous nature, or the silver particles have copper oxide growing at different angles on them, that would also explain the higher measured amorphousness

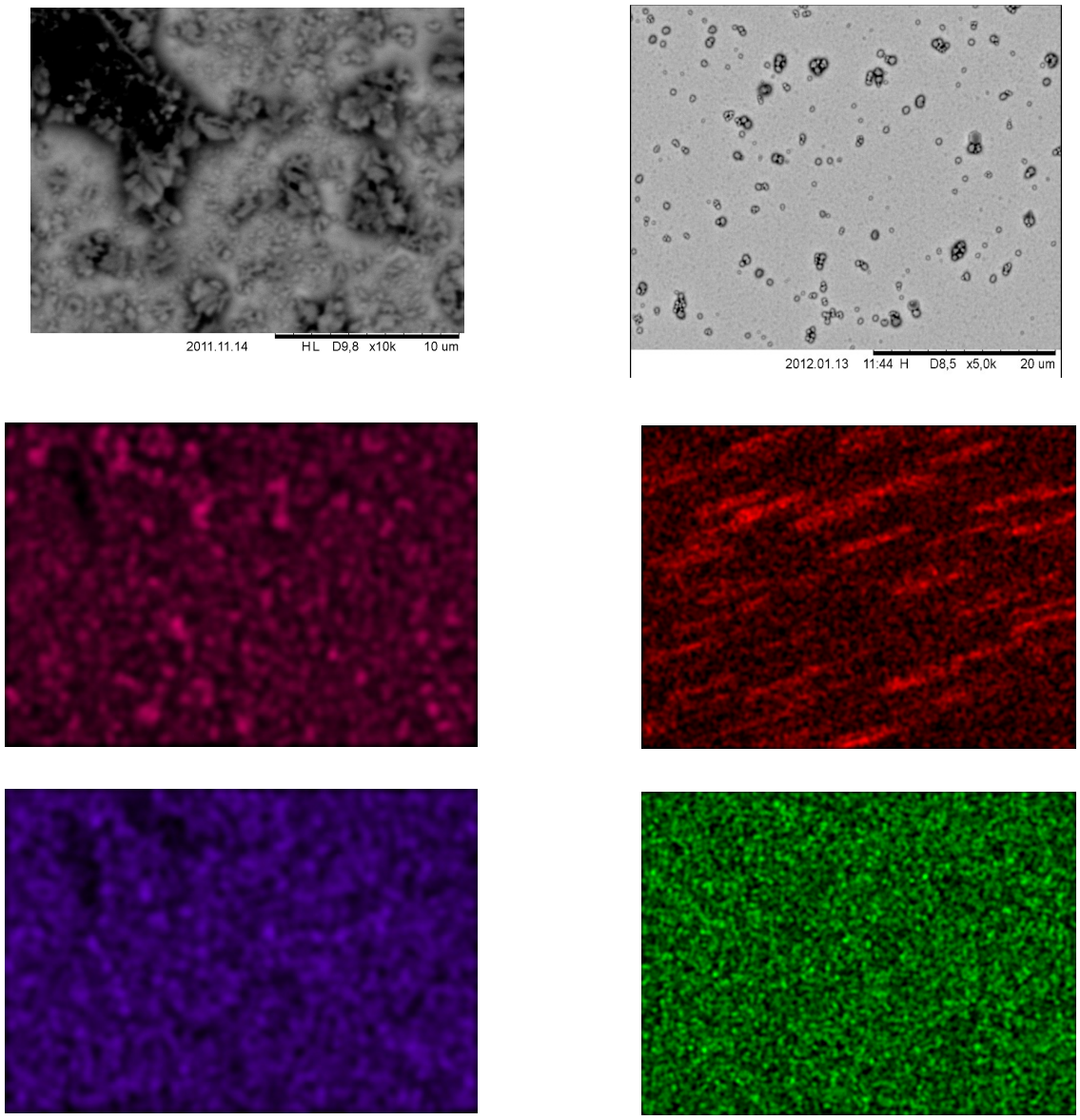

Figure 5.16: Elements distribution in films deposited at -0.3V (left) and -0.15V (right). From top to bottom: SEM image, silver map, and copper map. The magnification for the -0.3V films is twice the magnification for the -0.15V films

for the -0.8V/Cu film.

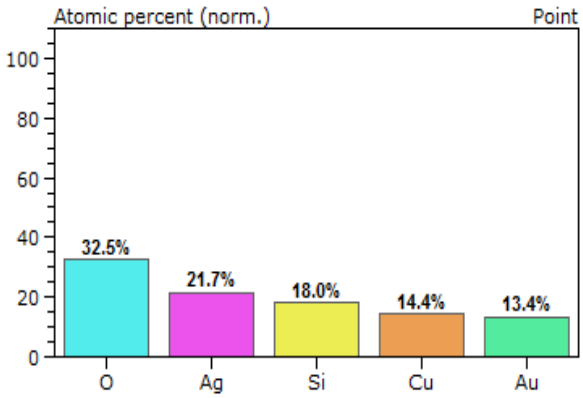

Figure 5.17: Quantitative analysis of elements found in a film deposited at -0.3V/Cu.

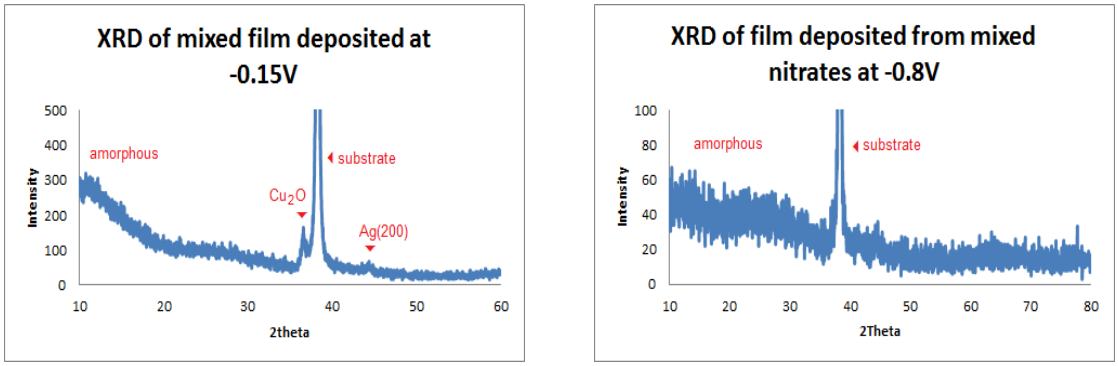

a) b)

Figure 5.18: (a) X-ray diffraction of film deposited at -0.15V/Cu from a solution of mixed nitrates. The peaks are found from [24, 31], (b) deposition at -0.8V/Cu from mixed nitrate solution.

5.5.4 Optical measurements of films from mixed nitrates

The films from cathodic deposition in mixed nitrate solutions did not yield any reflectance. This was expected considering their solid black visual appearance. The reason for this might be scattering caused by metal particles combined with absorbing oxides surrounding them.

5.6 Copper oxide films from nitrate solutions

The copper oxide films deposited at -0.8V and -0.3V vs Cu were very smooth and reflected light like known copper oxides. They were investigated with XRD and optical measurements to show they consisted of a mixture of Cu_2O and CuO.

5.6.1 XRD of copper oxide films

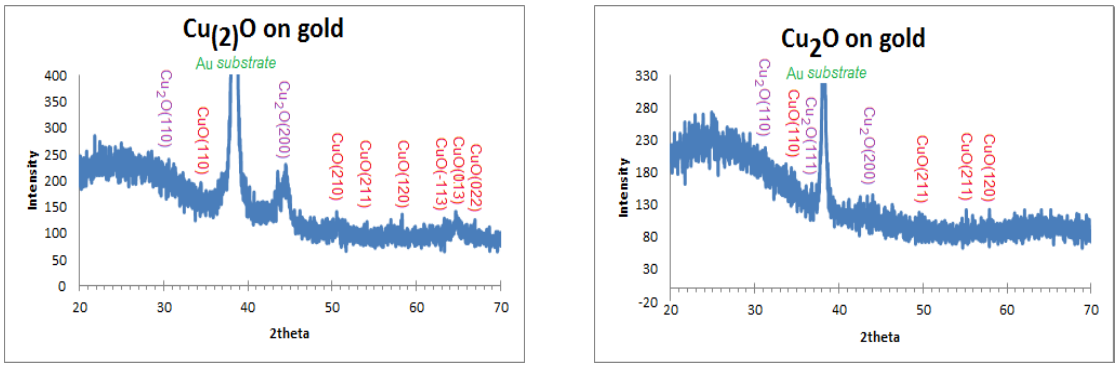

a) b)

Figure 5.19: (a) X-ray diffraction of film deposited at -0.3V/Cu from a solution of copper nitrate, (b) deposition at -0.8V/Cu from copper nitrate solution. The peaks are found from [24, 25].

XRD of a film deposited at -0.3V/Cu (Figure 5.19a) in a copper nitrate solution shows a mixture of CuO and Cu_2O peaks, indicating a film consisting of both copper oxides. Some co-deposition of the two oxides are likely, though the reported films deposited from alkaline buffered copper solutions were all Cu_2O. Likely the effect is a result of the nitrate in the solution allowing free copper ions rather than the suspended precipitate in the buffer solutions, and a resulting reaction looking something like the one for electrodeposition of zinc oxide from zinc nitrate solution, only at a smaller voltage. The deposition at 0.8V/Cu (Figure 5.19b) also show co-deposition of Cu_2O and CuO, and no peaks from metallic copper. The signal is however a bit noisy, so there might be hidden peaks. Along with the XRD results from the deposition at -0.3V/Cu it seems like oxides are deposited for the entire voltammetry well between 0 and -0.9V, but with different compositions of Cu_2O and CuO. More negative voltages seem to give more peaks from Cu_2O compared to smaller voltages, likely due to higher voltages attracting more positively charged copper ions while more strongly repelling hydroxide.

5.6.2 Optical measurements of copper oxides

The copper oxide film deposited at -0.8V/Cu showed a high absorption and a clearly defined band edge at 1.8-2.1eV (see Figure 5.20a)), as would be the case for a film of Cu_2O [23]. This is in line with the measurements from XRD where this film was found to contain this compound. The slightly reduced reflectance might be due to the measurement taking place within the band gap of CuO, though most of the reflectance spectrum indicates this film is mostly Cu_2O. The film deposited at -0.3V/Cu showed high absorbance, except for some reflectance at shorter wavelength (see Figure 5.20b)). The high absorbance suggests this measurement is within the band gap for CuO. This is all well in accordance with the findings in XRD, and it would seem that from nitrate solutions a mixture of Cu_2O and CuO is achieved at negative voltages, rather than the Cu_2O from alkaline buffer solutions.

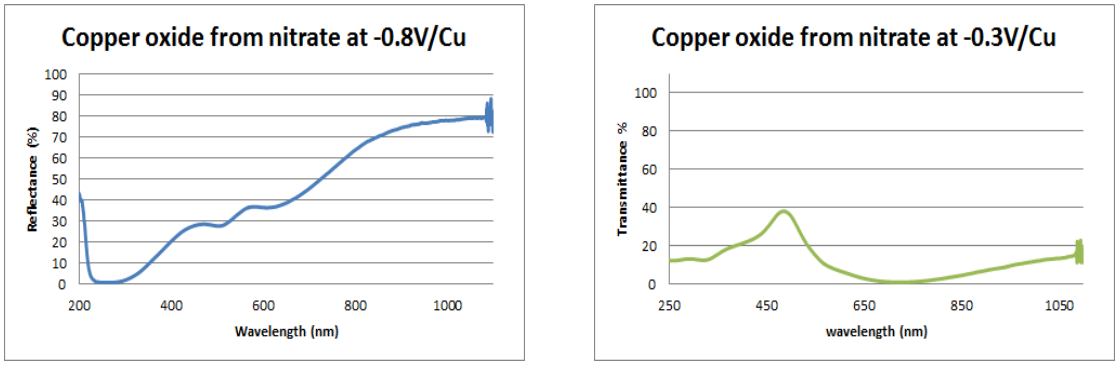

a) b)

Figure 5.20: Reflectance of copper oxide films deposited at (a) -0.8V vs Cu, and (b) at -0.3V/Cu. The short wavelength transmission in a) is an artifact of the spectrometer, according to prof. Gibson.

5.7 Anodic deposition from mixed nitrates

5.7.1 SEM and EDS/EDX

SEM was performed on three films deposited from nitrates mixed with NaOH that were different in deposition time only. The SEM images of Figure 5.21 shows the film in various stages of growth. As can be seen from Fig. 5.21, the number of small crystals increases as the film grows. The film deposited for 20 minutes are mostly bigger particles scattered about. The next stage, after 40 minutes when the stirring would be turned on, there has appeared a more noticeable layer with an uneven landscape and piles of material randomly placed on the surface. The film deposited for 180 minutes seems to be a thick layer of nanosized crystals in the smooth areas (see Figure 5.21), with the brown spots appearing as white in the SEM (see Figure 5.21d). For the film deposited for 40 minutes, EDS was performed. the EDS was focused on an area with a large lump of material. This lump can be seen to consist of copper silver and oxygen, all fairly evenly distributed in the lump, as seen in Figure 5.22. There are also some small concentrations of these materials outside the lump in the small crystals that can be seen. This shows great indication for the film to be silver copper oxide, either as $Ag_2Cu_2O_4$ or $Ag_2Cu_2O_3$. This can not be decided by EDS as the quantity of oxygen can not be accurately measured.

5.7.2 XRD

When XRD was run on the film that might be $AgCuO_2$ deposited for 180 minutes on PtSi substrate, peaks were found at 32°,34°,37°, 39°, 42°, 47°, 54°, 56°, 61°, 66°, and a large peak at 69° (see Figure 5.23). Then XRD of the PtSi substrate was done, and peaks were found at 39°, and 42°. The peaks at 32° and 34° correspond to literature values for $AgCuO_2$ [45]. And the literature peaks for $AgCuO_2$ and PtSi overlap at 42° [45]. The slight offset in the peak location in the figure is probably due to a small tilt of the sample in the $AgCuO_2$ plot, as a later plot showed the same offset as seen in the PtSi. The peak at 42° is bigger for the PtSi covered with $AgCuO_2$, indicating there might be some contribution from the film as well as the substrate. The same difference in peak height is not seen

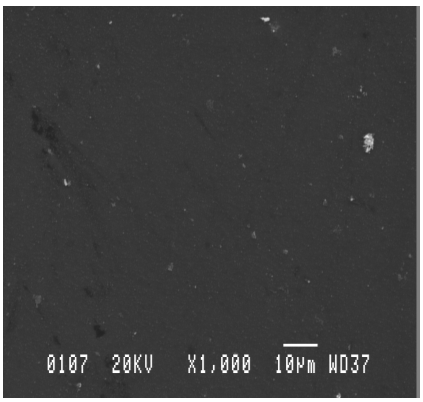

a)

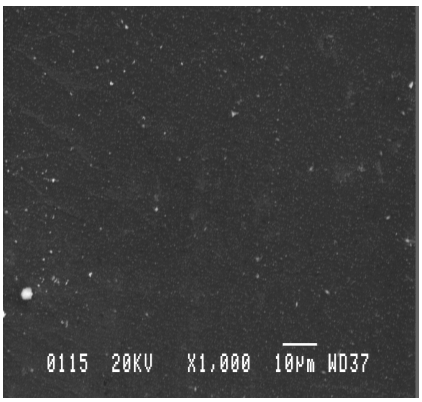

b)

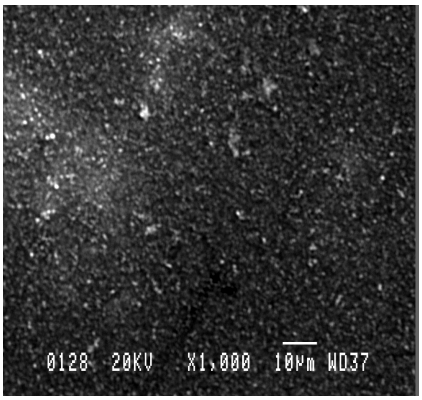

c)

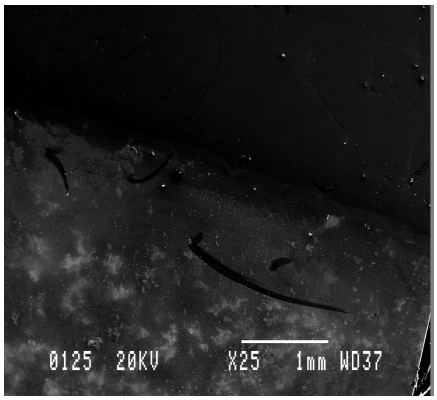

d)

Figure 5.21: Different stages of growth for a $Ag_2Cu_2O_4$ film from a solution of silver nitrate, copper nitrate and NaOH. The images (a)-(c) are of the same magnification, for 20 minutes(a), 40 minutes(b) and 180 minutes(c) deposition time. Image d) is an overview of the film deposited at 180min, white areas corresponding to the brown ones seen in the light microscope.

for the peak at 39°, where no silver copper oxide peak should be. The peaks at 37°, 56°, 61°, and 66° correspond to literature values reported in [44]. The peak at 54° might be due to AgO, which also has peaks in the 30°-40° range (32°,34°,37°,39°) [30]. These peaks overlap with the $AgCuO_2$, which is probably a result of the similarities in structure, and the 34° peak may be found in the slower scan rate plot in Figure 5.23b), but it is very thin. The $AgCuO_2$ peaks at higher angles are much larger and speaks in favor of this film being $AgCuO_2$ and not AgO. Another argument for this is the EDS plots, which indicated a similar distribution of silver and copper in the film. AgO from alkaline solutions should be deposited at the same voltage. If the solution was not well enough mixed early in the deposition there might have been some AgO and perhaps CuO deposited. To avoid this contamination it might be attempted to let the solution wait a while under stirring, perhaps until it had turned from green to brown/black, before deposition.
The large peak at 69° probably belongs to Si, though this peak is not seen on the PtSi scan. This

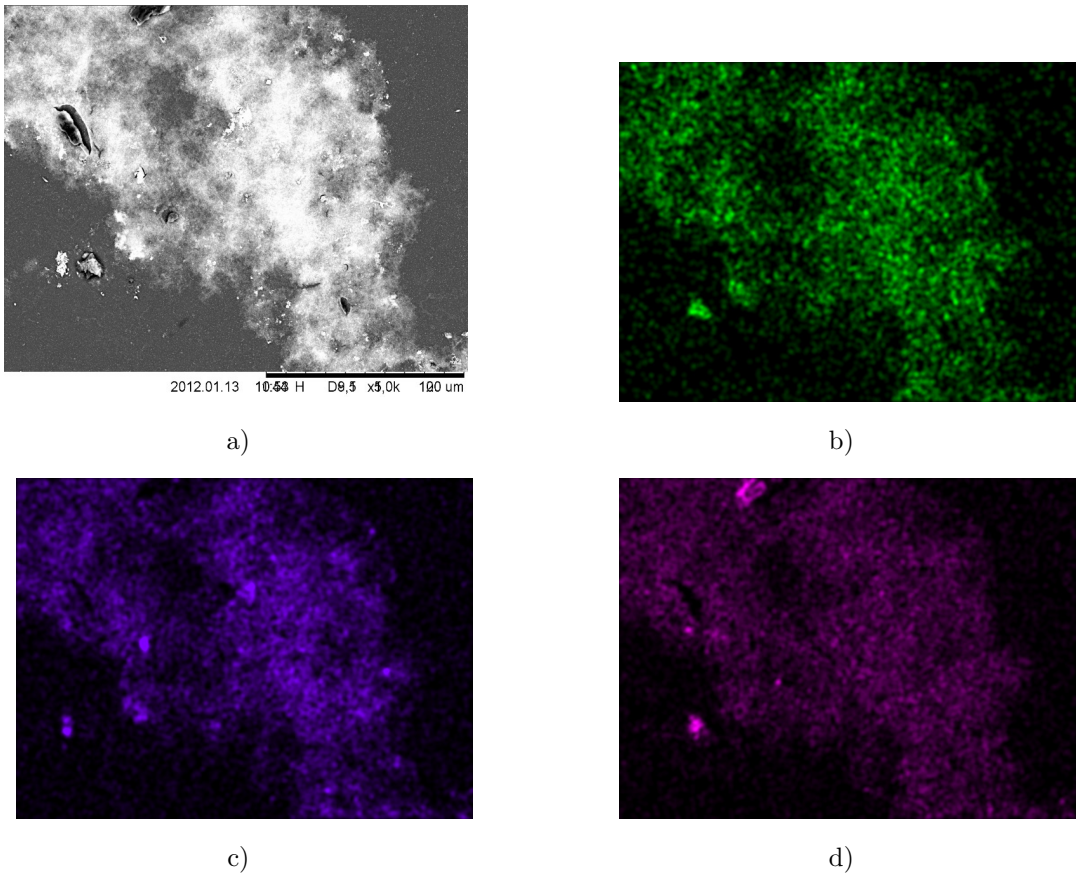

Figure 5.22: SEM image (a) of a structure on the film on PtSi deposited for 40 minutes, with maps of copper (b), silver(c) and oxygen(d) distribution in the same area.

indicates there is some damage to the PtSi layer covering Si for the sample with a film deposited on it. Such damage could be mechanical damage such as a scratch, chemical etching of the surface by NaOH or electrochemical etching due to the high voltage of the deposition. Of the three the electrochemical etching seems the most likely, especially considering the abrupt decrease in deposition current from 150μA to 20μA in the first minute of deposition. This early current might have been the stripping of Pt/PtSi from the surface before the layer of $AgCuO_2$ was deposited to protect the substrate.

5.7.3 Optical measurements

The reflected spectrums are shown in Figure 5.24c). They all show a large absorption at 200-350nm, and decreasing absorption with higher wavelength. Another bend in the curve appears at approximately 900nm. The thicker the films are the more they absorb. The plot from the thinnest film have the most defined peak at 300nm, and reflects about 50-90% of the light. The film deposited for 40 minutes reflects 40-80% of the light, and has the clearest bend at 900nm. The thickest film, deposited for 180 minutes, reflects only 20% of the light for most wavelengths, though the reflectance seems to increase a little with wavelengths larger than 800nm. These results indicate a band gap

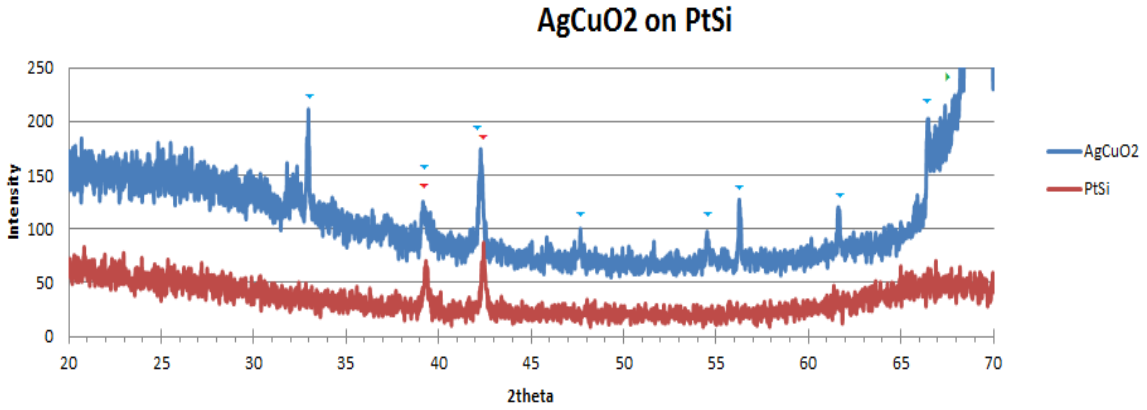

a)

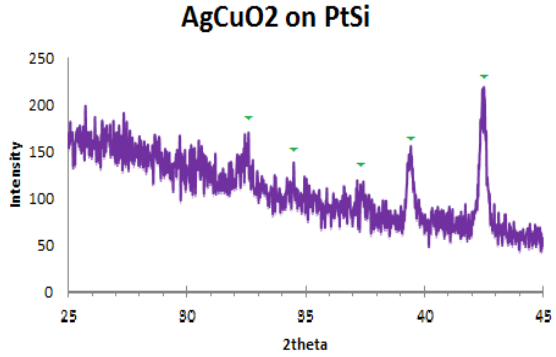

b)

Figure 5.23: a) X-ray diffraction of $AgCuO_2$ film on PtSi substrate (blue) and the PtSi substrate (red). b) $AgCuO_2$ on PtSi scanned at a slower rate between 2θ=25° and 2θ=45°. The arrows mark the mentioned peaks. c) Reflectance of silver copper oxide films deposited for 20min, 40min, and 180min.

of either 3.5eV or 1.45eV, or something outside the scale. Calculated band gaps for $AgCuO_2$ are between 0.2eV and 0.7eV [32]. These energies are outside the scale of the instrument. Due to the high absorption the range seen in this measurement might very well be inside the band gap, which means the band gap is less than 1.24eV, corresponding to 1000nm wavelength. The low reflectance might also be due to scattering, and the band gap is 3eV, like in the ZnO film. This is unlikely given the smooth appearance of the film, it is also not white, like the ZnO film was. There is a possibility that the extra edge is a result of impurities in the film due to the possible etching of the PtSi from high voltage deposition.

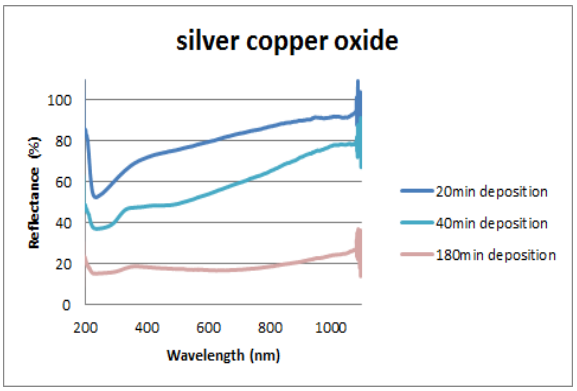

Figure 5.24: Reflectance of silver copper oxide films deposited for 20min, 40min, and 180min.

6. Conclusions

Electrodeposition of oxides can be performed both at anodic and cathodic voltages. pH seems to be important for depositions at anodic deposition, and then the substrate can not be gold. Deposition of mixed oxides require the individual metal oxides it should contain to deposit in a similar manner, but these do not always deposit well under the same conditions. This means individual oxides are easier to deposit than mixed. For mixed oxide deposition the deposition voltage should allow for the noblest of the metals to be oxidized.

6.1 Zinc oxide

Zinc oxide was successfully deposited at -1.0V and -0.8V vs. AgCl. Stirring was required to avoid formation of nanoflowers. A film deposited at -0.8V had band gap between 3.2eV and 3.5eV. XRD proved this film to be polycrystalline.

6.2 Silver oxide

Silver oxide proved difficult to deposit. Cathodic deposition only gave metallic silver, and anodic deposition proved difficult as the film had trouble sticking to the surface. A film deposited anodically on a copper substrate was made, though it was contaminated by copper.

6.3 Copper oxide

A film deposited at -0.8V/Cu was deposited and characterized and appeared to be polycrystalline Cu_2O in all measurements except XRD, where it looked amorphous.

6.4 Silver copper oxide

This study has performed the first successful electrodeposition of a film of $Ag_2Cu_2O_4$. This can be performed on a PtSi substrate from a solution of milli-molar concentration of silver nitrate, copper nitrate and NaOH with a 0.9V anodic voltage vs. a silver metal counter/reference electrode. The process produces a polycrystalline film consisting of silver, copper, and oxygen with the XRD peaks corresponding to previously reported $Ag_2Cu_2O_4$. The film shows very high light absorbance quality. Electrodeposition with cathodic voltages lead to metallic silver.

7. Future studies

For future studies, other voltages should be tested. For a more homogeneous deposition process with less precipitation, a flow reactor mixing the solutions could be tested, or a buffered solution where the OH^- is slowly released. Also, other substrates and different concentrations can be tried, especially ITO covered glass would allow for transmission measurements. And finally, production of a solar cell of silver copper oxide and zinc oxide could be attempted.
It is possible that depositing an AgO film and encouraging it to take up copper, for example by submersion in a high concentration copper containing solution for some time might replace the Ag^{III} with Cu^{III}, as in rection equation 7.1.

$$Ag^{I}Ag^{III}O_2 + Cu^{+} \rightarrow Ag^{I}Cu^{III}O_2 + Ag^{+} \tag{7.1}$$

Comparing the reduction potentials of silver and copper clearly shows that copper is more easily oxidized than silver.

$$Ag^{2+} + e^{-} \rightarrow Ag^{+} \qquad E_0 = 1.99\text{V/NHE} \tag{7.2}$$

$$Cu^{2+} + e^{-} \rightarrow Cu^{+} \qquad E_0 = 0.16\text{V/NHE} \tag{7.3}$$

Bibliography

[1] John Twildell & Tony Weir, *Renewable Energy Resources*, second edition, Taylor & Francis, 2006, ISBN 0-419-25330-0.

[2] M.A. Green et al. *Prog. Photovolt: Res. Appl.*, 2007, 15:425430

[3] M. Izaki, T. Omi *Appl. Phys. Lett* 68 (1996) 17

[4] M. Izaki, T.Omi *J.Electrochem. Soc.*, Vol. 143, No. 3 (1996) L53-L55

[5] S.Peulon, D. Lincot *J. Electrochem. Soc.*, vol. 143, No.3, (1998), 864-874

[6] D. Lincot, S. Peulon *Adv. Mater* 8(1996) No 2

[7] S.S. Jeong, A. Mittiga, E. Salza, A. Masci, S. Passerini, *Electrochimica Acta* 53 (2008) 2226-2231

[8] B.D. Yuhas, Pd. Yang, *J. Am. Chem. Soc.* 2009, 131, 37563761

[9] K. Akimoto et al. / *Solar Energy* 80 (2006) 715722

[10] Katayama, J.; Ito, K.; Matsuoka, M.; Tamaki, *J. Appl. Electrochem.* 2004, 34, 687.

[11] B.G. Streetman, S.K. Banerjee, *Solid State Electronic Devices* 6th ed. Pearson int. ed., 2010, ISBN 13: 978-0-13-245479-7

[12] P. Bhattacharya, *Semiconductor Optoelectronic Devices* 2nd ed., Prentice Hall Inc., 1997, ISBN 0-13-495656-1

[13] S.R. Elliot, *The Physics and Chemistry of Solids*, 2000, ISBN-13: 978-0-471-98194-7

[14] S.J. Pearton et al. *Progress in Materials Science* 50 (2005) 293340

[15] M.A. Green, *Solar Cells, Operating Principles, Technology and System Applications* Prentice Hall Inc., 1982, ISBN 0-13-82270

[16] K. L. Chopra, P. D. Paulson, and V. Dutta, *Prog. Photovolt: Res. Appl.* 2004; 12:6992

[17] D. Lincot *Thin Solid Films* 487 (2005)40-48

[18] T. Pauporte, D. Lincot, *Electrochimica Acta* 45 (2000) 3345-3353

[19] K.M. McPeak et. al., *Chem Mater* 22 (2010)6162-6170

[20] Z.H. Gu, T.Z. Fahidy *J. Electrochem. Soc.*146 (1) 156-159 (1999)

[21] M. Fahome et al. *Solar Energy Materials & Solar Cells* 90 (2006) 1437-1444

[22] Gordon Aylward and Tristan Findlay *SI chemical data* 5th ed., 2002, John Wiley & Sons Australia Ltd, ISBN-13 978 0 470 800444 7

[23] A. E. Rakhshani *Solid-State Ekctronics* Vol. 29. No. 1. pp. 7-17, 19X6

[24] R.P. Wijesundera, M. Hidaka, K. Koga, M. Sakai, W. Siripala*Thin Solid Films* 500 (2006) 241 246

[25] R. P. Wijesundera,*Semicond. Sci. Technol.* 25 (2010) 045015

[26] E.W.Bohannan, M.G. Shumsky, J.A. Switzer, *Chem. Mater.* 1999, 11, 2289-2291

[27] J.K. Barton et al., *Chem. Mater.*, 2001, 13, 952-959

[28] J. Curda, W. Klein, H. Liu, M. Jansen, *Journal of Alloys and Compounds* **338** (2002) 99103

[29] Y. Ida et al.,*Chem. Mater.*, Vol. 20, No. 4, 2008

[30] B.E. Breyfogle et al., *J. Electrochem. Soc.*, Vol. 143, No.9, 1996

[31] G.M. de Oliveira et al., *Journal of Electroanalytical Chemistry* 578 (2005) 151158

[32] J. Feng et al. / Solid State Communications 149 (2009) 1569-1573

[33] J. Curda, W. Klein, and M. Jansen, *Journal of Solid State Chemistry* **162**, 220-224 (2001)

[34] Munoz-Rojas et al./ J. Phys. Chem. B 2005, 109, 6193-6203

[35] P. Gomez-Romero, E. Tejada-Rosales, M.R. Palacin, Angew. Chem. Int. Ed. Engl. 38 (1999) 524525.

[36] D. Munoz-Rojas et al. / Electrochemistry Communications 4 (2002) 684689

[37] J.F.Pierson et al. *Applied Surface Science* 253 (2006),1484-1488

[38] Southampton Electrochemistry Group,*Instrumental Methods in Electrochemistry*, 1985, Ellis Hornwood Limited, ISBN 0-85312-875-8

[39] P.H. Rieger, *Electrochemistry*, 2nd ed., Chapman & Hall Inc.,1994, ISBN 0-412-04391-2

[40] http://voltammetry.net/pine/wavenow/specifications

[41] E. M. Slayter, H. S. Slayter, *Light and Electron Microscopy*, 1992, Cambridge University Press, ISBN 0-521-32714-8

[42] A.J. Garrat-Reed, D.C. Bell, *Energy-Dispersive X-Ray Analysis in the Electron Microscope*, 2003, BIOS Scientific Publishers Ltd, ISBN 1 85996 109 6

[43] A Liu et al., *Chem. Eng. Comm.*, 198, 494503, 2011

[44] C.D. May, J.T. Vaughey *Electrochemistry Communications* 6 (2004) 10751079

[45] Munoz-Rojas et al., *Inorganic Chemistry*, Vol. 49, No. 23, 2010